# Design and Optimization of Heterojunction-Based FET Device for Low-Power Bio-sensing Application

**Abinet Bekele Mamo**

A Thesis Submitted to

Department of Electronics and Communication Engineering,

College of Electrical Engineering and Computing

Presented in Partial Fulfillment of the Requirement for the Master of Science Degree in Electronics and Communication Engineering

Office of Graduate Studies

Adama Science and Technology University

June, 2025

Adama, Ethiopia

# Design and Optimization of Heterojunction-Based FET Device for Low-Power Bio-sensing Application

**Abinet Bekele Mamo**

Major advisor: **Dr. Avtar Singh**

Co-Advisor: **Dr. Demissie Jobir**

A Thesis Submitted to the Department of Electronics and Communication Engineering,

College of Electrical Engineering and Computing

Presented in Partial Fulfillment of the Requirement for the Master of Science Degree in Electronics and Communication Engineering

Office of Graduate Studies

Adama Science and Technology University

June, 2025

Adama, Ethiopia

# DECLARATION

I hereby declare that this Master Thesis entitled **"Design and Optimization of Heterojunction-Based FET Device for Low-Power Bio-sensing Application"** is my own work. That is, it has not been submitted for the award of any academic degree, diploma, or certificate in any other university. All sources of materials that are used for this thesis have been duly acknowledged through citation.

| ______________________ | ______________ | ______________ |
|---|---|---|
| Name of Student | Signature | Date |

# RECOMMENDATION

We, the advisors of this thesis, hereby certify that we have read the revised version of the thesis entitled **"Design and Optimization of Heterojunction-Based FET Device for Low-Power Bio-sensing Application"** prepared under our guidance by Abinet Bekele Mamo submitted in partial fulfillment of the requirements for the degree of Master of Science in Electronics and Communication Engineering. Therefore, we recommend the submission of the revised version of the thesis to the department following the applicable procedures.

| ___________________________ | ________________________ | ________________ |
| --- | --- | --- |
| Major Advisor name | Signature | Date |
| ___________________________ | ________________________ | ________________ |
| Co-advisor name | Signature | Date |

# APPROVAL PAGE OF M.SC. THESIS

We, the advisors of the thesis entitled **"Design and Optimization of Heterojunction-Based FET Device for Low-Power Bio-sensing Application"** and developed by Abinet Bekele Mamo hereby certify that the recommendation and suggestions made by the board of examiners are appropriately incorporated into the final version of the thesis.

| | | |
|---|---|---|
| Major Advisor | Signature | Date |
| Co-advisor | Signature | Date |

We, the undersigned, members of the Board of Examiners of the thesis by Abinet Bekele Mamo, have read and evaluated the thesis entitled **"Design and Optimization of Heterojunction-Based FET Device for Low-Power Bio-sensing Application"** and examined the candidate during open defense. This is, therefore, to certify that the thesis is accepted for partial fulfillment of the requirement of the degree of Master of Science in Electronics and Communication Engineering.

| | | |
|---|---|---|
| Chairperson | Signature | Date |
| Internal Examiner | Signature | Date |
| External Examiner | Signature | Date |

Finally, approval and acceptance of the thesis are contingent upon the submission of its final copy to the Office of Postgraduate Studies (OPGS) through the Department Graduate Council (DGC) and School Graduate Committee (SGC).

| | | |
|---|---|---|
| Department Head | Signature | Date |
| College Dean | Signature | Date |
| Office of Postgraduate Studies, Dean | Signature | Date |

# ACKNOWLEDGMENT

Above all, I thank Almighty God for His endless grace, strength, and guidance throughout this journey.

I am deeply grateful to my main advisor, Dr. Avtar Singh, for his invaluable support, insightful guidance, and continuous encouragement throughout the course of this research. My sincere thanks also go to my co-advisor, Dr. Demissie Jobir, for his thoughtful feedback and constructive suggestions, which have significantly enriched the quality and depth of this work.

I wish to express my heartfelt appreciation to my family for their unconditional love, prayers, and unwavering support. Their constant belief in me has been the foundation of my strength and perseverance throughout my academic journey.

I extend my heartfelt appreciation to Yohannes Melese, whose consistent support, patience, and encouragement have been a constant source of strength and motivation. I am also deeply grateful to my dear friends, whose kindness, shared experiences, and consistent moral support helped me stay focused and resilient during challenging times. Their presence made this journey not only bearable but truly meaningful.

Finally, I extend my sincere thanks to all the faculty members of the Department of Electronics and Communication Engineering at ASTU, Adama, Ethiopia, for their guidance, support, and cooperation during my studies.

# TABLE OF CONTENT

# LIST OF FIGURES

# LIST OF TABLES

# ABSTRACT

*Addressing the limitations of traditional biosensors, this work presents a high-sensitivity, low-leakage HTFET architecture using advanced material and structural innovations. A source-engineered TFET is analyzed by comparing conventional TFETs with Indium Phosphide (InP) drain TFETs, significantly reducing ambipolar leakage. A comparative analysis of Indium Antimonide (InSb) and Germanium (Ge) as source materials on InP and Si drains confirms superior InP drain performance. A Ge-source extended structure with a highly doped Si pocket at the source-channel interface improves ON-state current (I_ON). Further enhancements include a dielectric pocket at the channel-drain junction to suppress ambipolar current and an InSb source pocket for higher drive capability. Electrical characterization of vertical TFETs with SiGe pockets supports their suitability for biosensing applications.Two dielectric-modulated FET biosensors are designed: (1) InAs/InGaAs HTFET and (2) Ge split-source HTFET, both simulated using Silvaco Atlas TCAD. The heterojunction interfaces and narrow-bandgap materials enhance tunneling sensitivity. The InAs/InGaAs HTFET achieves I_ON of* **$4.355 \times 10^{-5}$ A/μm**, *I_OFF of* **$5.117 \times 10^{-14}$ A/μm,** *and an I_ON/I_OFF ratio of* **$8.51 \times 10^{9}$,** *with a subthreshold swing (SS) of* **18.2 mV/dec**, *ensuring energy-efficient biosensing. Sensitivity evaluations for streptavidin, ferricytochrome, keratin, and gelatin demonstrate superior drain current sensitivity compared to the Ge Split-Source HTFET. This work addresses conventional FET biosensor limitations, advancing high-sensitivity, low-power sensing for healthcare diagnostics, environmental monitoring, and industrial automation. The findings emphasize material selection, heterojunction engineering, and structural optimization for biosensor performance improvement.*

**Keywords:** Heterojunction-based FET, low power sensing application, FET-based sensors.

# ACRONYMS

| | |
|---|---|
| CMOS | Complementary Metal-oxide Semiconductor |
| FET | Field Effect Transistor |
| HFET | Heterojunction Field Effect Transistor |
| 2DEG | Two-dimensional Electron Gas |
| TCAD | Technology computer-aided design |
| MOSFET | Metal Oxide Semiconductor Field Effect Transistor |
| TFETs | Tunnel Field Effect Transistor |
| BTBT | Band To Band Tunneling |
| NC-TFETs | Negative Capacitance Tunnel Field-Effect Transistors |

# CHAPTER 1 INTRODUCTION

## 1.1 Background of the Study

Over the past three centuries, technological innovation has profoundly transformed modern society, with electronic devices becoming integral to daily life in developed nations. Central to this digital revolution is the continuous miniaturization of electronic components, particularly the metal-oxide-semiconductor field-effect transistor (MOSFET), which has long served as the foundational element in logic and memory circuits.

In accordance with Moore's Law, the number of transistors on a microchip has historically doubled approximately every two years, resulting in exponential improvements in computational power. However, this trend has shown signs of slowing the boundaries of geometric scaling started to show by 2012, when the 22 nm technology node was introduced, and more clearly at the 14 nm and 10 nm nodes.

To extend the trajectory of Moore's Law, the semiconductor industry has increasingly focused on innovative device architectures and materials. These include multi-core processing, novel transistor designs, and heterogeneous integration. As transistor dimensions shrink to just a few nanometers, new paradigms in device design are essential to maintain energy efficiency, computational speed, and fabrication feasibility.

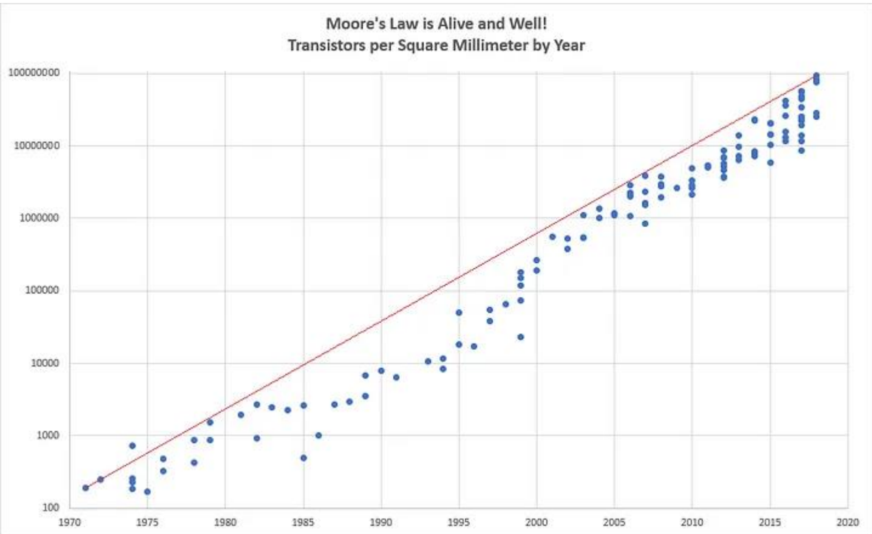


*Figure 1.1Moore's Law*

Despite these advances, conventional MOSFET architectures are now constrained by short-channel effects (SCEs), high leakage currents, and the inability to achieve subthreshold swing (SS) values below the thermionic limit of 60 mV/dec. These limitations hinder performance in ultra-scaled and low-power applications, prompting a shift toward alternative transistor designs.

Due to the performance limitations of MOSFETs at reduced dimensions, the semiconductor industry has been actively exploring alternative technologies. According to the needs of the semiconductor industry today, researchers have proposed innovative devices with good prospects when compared to MOSFETs in terms of performance. A novel transistor idea that works with CMOS technology, the TFET has been suggested as having an SS below the MOSFET limit. This is made possible by the fact that the TFET uses quantum mechanical BTBT as the carrier injection mechanism rather than thermionic emission. In 1978, the fundamental TFET structure was originally put forth as a “surface channel tunnel.” (Verreck et al., 2016).

The fundamental architecture of a Tunnel Field-Effect Transistor (TFET) is similar to that of a traditional MOSFET, with two contact regions and an inherent or mildly doped channel region layered with a gate electrode and a gate dielectric. The TFET, in contrast to the MOSFET, has a p-i-n structure with oppositely doped source and drain regions. The source of a p-type TFET (pTFET) is n-type, while that of an n-type TFET (nTFET) is p-type (Verreck et al., 2016). While they hold promise for low-power applications, Tunnel Field-Effect Transistor (TFETs) have significant drawbacks, such as poor ION and ambipolar behavior in current conduction.

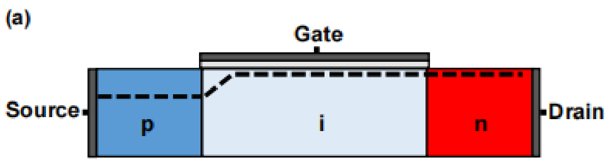


*Figure 1.2TFET Structure*

In recent years, heterojunction-based field-effect transistors (FETs) have emerged as a promising approach to overcome these constraints. By integrating two semiconductor materials with different bandgaps, heterojunctions offer several advantages, including enhanced carrier mobility, reduced scattering, and the ability to tunable energy band alignments for specific applications. Depending on the band alignment at the interface, heterojunctions are classified into Type-I (straddling gap), Type-II (staggered gap), and Type-III (broken gap), each offering distinct benefits for applications ranging from optoelectronics to sensing and high-speed logic (Ghadimi Avval et al., 2018).

To further enhance performance, heterojunction TFETs have been proposed that combine the benefits of bandgap engineering with advanced materials and device physics. These structures utilize high-k dielectrics (e.g., $HfO_2$) and charge plasma techniques, replacing traditional doping with electrostatic carrier generation through metal work-function engineering. This innovation eliminates the need for abrupt junctions and ensures uniform carrier distribution, improving both reliability and sensitivity at nanoscale dimensions (Farkoush & Dideban, 2020)

### 1.1.1 Biosensors as promising Application of TFETs

Biosensors are analytical devices that integrate a biological recognition element such as an enzyme, antibody, or nucleic acid with an electronic transducer to detect and quantify specific analytes. These devices function by sensing and recording environmental changes caused by chemical or genetic substances. The transducer transforms the biological component's selected interaction with the target analyte into a detectable signal, usually electrical in nature. Biosensors are therefore vital instruments in a variety of domains, including biotechnology, environmental monitoring, and healthcare, as they allow the precise identification of biomolecules, infections, and environmental pollutants.

Among various biosensing platforms, electrochemical field-effect transistor (FET)-based biosensors have garnered significant attention due to their numerous advantages, including label-free detection, compactness, rapid response, cost-effective fabrication, and compatibility with CMOS technologies. These sensors are particularly effective for real-time monitoring of a wide range of biomolecules such as proteins, DNA, pathogens, and volatile organic compounds (VOCs) which are critical in disease diagnostics and environmental surveillance (Poorna Sundari & Lakshmi Priya, 2024).

Advanced sensing technologies, especially those that employ material systems like InAs/InGaAs, InSb, AlGaN, and other III-nitride semiconductors, have demonstrated a great deal of potential using heterojunction-based FETs. These heterostructures enable high electron mobility without the need for traditional doping methods by forming a two-dimensional electron gas (2DEG) at the interface. (Hong and others, 2021). Additionally, by maximizing the contact between the target analytes and the detecting surface, these biosensors' sensitivity and selectivity can be customized.

Since the advent of the first enzyme-based biosensor in 1962, the technology has expanded to encompass various detection mechanisms and biological recognition elements. Biosensors are typically categorized by their transduction methods electrochemical, optical, piezoelectric, and calorimetric as well as by the type of biorecognition element they employ, including enzymes, antibodies, and nucleic acids (Reddy & Panda, 2020).

In practical applications, biosensors play a pivotal role in healthcare (e.g., continuous glucose monitoring, early disease detection), environmental protection (e.g., pollutant tracking, air and water quality assessment), and industrial processes (e.g., toxin detection, process control). The timely detection of hazardous substances is essential for preventing health risks and ensuring public safety. Additionally, biosensors are increasingly employed in breath analysis to detect biomarkers indicative of metabolic and respiratory disorders (Hong et al., 2021).

In response to these evolving needs and technological opportunities, this thesis focuses on the design and optimization of a low-power, heterojunction-based FET biosensor using advanced Technology Computer-Aided Design (TCAD) simulation tools. By integrating wide-bandgap semiconductors, two-dimensional materials, and engineered heterostructures, the proposed biosensor aims to achieve superior sensitivity, minimized power consumption, and scalable integration. Through this research, next-generation biosensing technologies with a broad range of applications in industrial safety, environmental monitoring, and healthcare diagnostics are being developed.

**Components of a Biosensor**

**Analyte:** The analyte is the target substance to be detected or measured by the biosensor. Examples include glucose, ammonia, alcohol, lactose, or other chemical or biological molecules present in a sample. The analyte interacts with the bioreceptor to initiate the sensing process, making it the focal point of detection.

**Bioreceptor:** A biological element or macromolecule known as a bioreceptor is capable of specifically identifying and attaching itself to the target analyte. Enzymes, antibodies, cells, deoxyribonucleic acid (DNA or RNA), and microbial products are examples of common bioreceptors. A signal is produced when the bioreceptor and analyte interact; this signal could take the form of light, heat, a change in pH, a variation in charge, or other observable phenomena. The sensitivity and selectivity of the biosensor depend on this interaction.

**Transducer:** The bio-recognition event that is, the interaction between the bioreceptor and analyte is transformed into a quantifiable signal, usually electrical, by the transducer, a crucial part of the biosensor. Signalization is the process that changes one type of energy into another. The number of analyte-bioreceptor interactions determines how many optical, electrical, or other signals the transducer produces. Transducers are categorized as electrochemical, optoelectronic, thermal, electronic, or gravimetric based on how they work, and each is appropriate for a particular biosensing application.

**Electronics:** The signal generated by the transducer is processed by the electronics component. It transforms the transducer's electrical output into a digital format for additional examination after amplifying it. After processing, this signal is ready for display, guaranteeing that the presence or concentration of the analyte is accurately represented. Reliable data interpretation and improved signal quality are made possible by the electronics system.

**Display:** Depending on the needs of the application, the display unit shows the processed data in a manner that is easy for users to understand, such as tables, graphs, or numerical figures. Users can easily interpret the biosensor's response by using output devices such as computers, printers, or screens. Regarding transducer and electronics systems, the display guarantees that the end user may access and act upon the results.

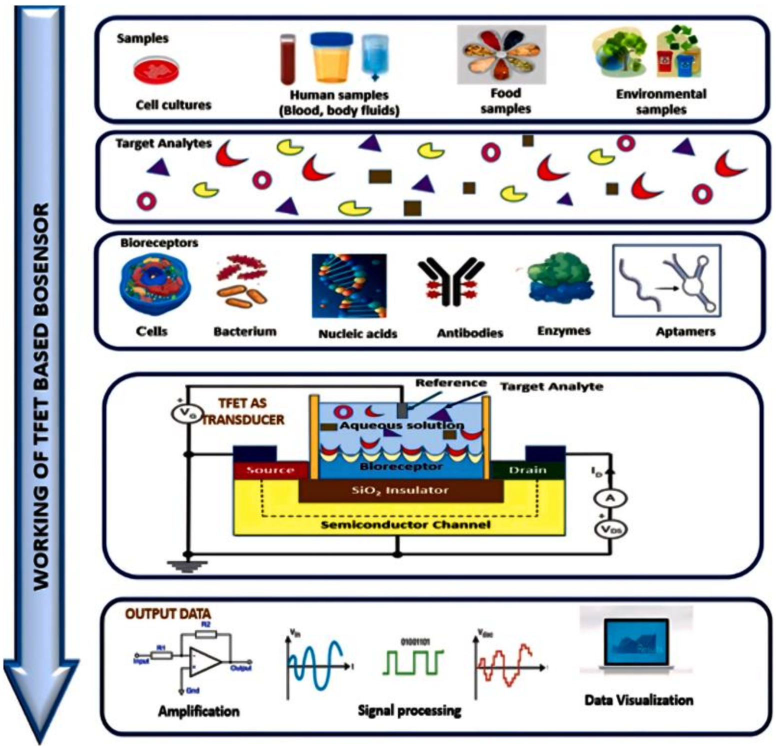


*Figure 1.3 Architecture and operational mechanism of TFET-based biosensors*

**Characteristics of Biosensors**

To design a highly effective and efficient biosensor system, specific static and dynamic characteristics are essential. These attributes enhance the performance of biosensors for commercial applications, ensuring reliability and accuracy. Below is a rewritten description of the key characteristics of biosensors.

1. **Selectivity:** The ability of the bioreceptor to recognize a particular target analyte in a complex sample that contains contaminants or interfering compounds is determined by its selectivity, which is a crucial property. By binding only to the desired analyte, a highly selective bioreceptor reduces false positives and improves the specificity of the biosensor, ensuring reliable detection.

2. **Sensitivity:** The term “sensitivity” describes a biosensor’s capacity to identify an analyte’s lowest concentration, which is usually in the range of nanograms per milliliter (ng/mL). For applications that need early detection, such environmental monitoring or medical diagnostics, it makes it possible to precisely identify analyte traces in a sample, even at low dosages.

3. **Linearity:** The precision of the biosensor’s response over a range of analyte concentrations is reflected in linearity. Reliable quantification is made possible by a linear response, which approximates a straight line and guarantees that the measured signal is proportionate to the analyte concentration. Increased linearity increases substrate detection accuracy.

4. **Response Time:** Response time is defined as the duration required for the biosensor to achieve 90 to 95% of its final output signal after exposure to the analyte. A shorter response time is essential for real-time monitoring applications, enabling rapid detection and timely decision-making.

5. **Reproducibility:** Reproducibility includes the accuracy (capacity to yield findings that are near to the true value) and precision (ability to give consistent results across many measurements of the same sample) of the biosensor. When evaluating the same sample repeatedly, a repeatable biosensor reliably produces consistent results, guaranteeing its dependability in real-world applications.

6. **Stability:** For biosensors used in situations involving continuous monitoring, stability

is an essential feature. It speaks to the biosensor's ability to withstand changes in the environment, both internal (like bioreceptor deterioration) and external (such variations in pH or temperature). In order to provide constant performance during extended use, stability is determined by the bioreceptor's affinity (the strength of analyte binding) and resistance to degradation over time.

### 1.1.2 Needs of Biosensor

The demand for biosensors has grown due to the need for rapid, accurate, and cost-effective biomolecule detection in medical diagnostics, food safety, environmental monitoring, and biodefense. Biosensors enable real-time monitoring, portability, and point-of-care testing, improving early disease detection and reducing healthcare costs. The need for biosensors is critical given the increase in bio attacks, such as the coronavirus pandemic and HIV, as well as the possibility of biological warfare utilizing harmful bacteria or viruses. By being integrated into healthcare, defense, and environmental systems, these tools are essential for promptly identifying biohazards, facilitating early response, and guaranteeing public health and safety.

## 1.2 Statement of the Problem

Extensive research into enhanced transistor technologies has been give rise to by the growing need for high-performance and energy-efficient devices in applications including biomedical diagnostics, environmental monitoring, and the Internet of Things (IoT). Despite their maturity, traditional MOSFETs' energy efficiency is limited by the thermionic limit of subthreshold swing (SS), which is restricted at 60 mV/decade.

The use of band-to-band tunneling by Tunnel Field-Effect Transistors (TFETs), which allows for ultra-low power operation with sub-60 mV/decade SS, has made them a possible substitute. The adoption of these devices in high-speed and high-performance systems is hindered by their intrinsically low ON-state current (ION).

Heterojunction-based devices like InAlN/GaN High Electron Mobility Transistors (HEMTs), which provide a compelling solution by striking a favorable balance between high ION and low OFF-state leakage current (IOFF), have being investigated by researchers in order to overcome this difficulty. Strong current driving capabilities are made possible by the high-density two-dimensional electron gas (2DEG) that is created at the InAlN/GaN interface, which greatly increases carrier mobility (Peng Cui et al., 2021).

Further advancing this direction, heterojunction-based Field-Effect Transistors (FETs) have been proposed as a novel solution to overcome the limitations of conventional sensor devices, which often face issues like high power consumption, limited sensitivity, and environmental instability. By utilizing engineered heterointerfaces, these devices enable precise control over band alignment and facilitate 2DEG formation, resulting in enhanced sensitivity, improved carrier transport, and superior energy efficiency (Liu et al., 2021).

In summary, while TFETs provide a pathway to ultra-low power operation, integrating heterojunction engineering such as in InAlN/GaN HEMTs or heterojunction FET biosensors offers a comprehensive solution that combines low power consumption with high performance, making them highly suitable for next-generation sensing and computation platforms.

## 1.3 Motivation

The development of heterojunction-based biosensors is motivated by the need to overcome the limitations of conventional biosensors while capitalizing on the unique advantages of heterojunction TFETs. By offering superior sensitivity, energy efficiency, and compatibility with modern technologies, these biosensors have the potential to transform biosensing applications, addressing critical societal needs in health, environment, and beyond.

## 1.4 Objectives

### 1.4.1 General Objective

The main objective of this thesis is to design and perform the DC parametric analysis of heterojunction-based transistor architecture and optimize the performance of the proposed structure for low-power bio-sensing applications.

### 1.4.2 Specific Objectives

1. To design a band-engineered heterojunction-based FET architecture and simulate its performance using the TCAD tool
2. To evaluate the electrical characteristics of the proposed design, focusing on- current, leakage current, subthreshold slope, and the device switching ratio.
3. To enhance the device's performance by adjusting parameters such as doping concentration, graded channel, dielectric material, pocket implantation, and similar factors.

4. Implement the proposed FET device design to be suitable for low-power bio-sensing applications.

## 1.5 Significance of the Study

Designing and optimizing heterojunction-based FET devices for low-power biosensing applications is the main emphasis of this important study. Through the use of cutting-edge heterojunction topologies and creative simulation techniques, the study seeks to address the sensitivity, power consumption, and operational dependability issues with conventional FETs. This study offers workable ways for enhancing electrical performance metrics including ON current, leakage current, and switching ratios by carefully integrating material properties. The results provide the foundation for next developments in low-power electronics while addressing pressing needs in industrial automation, biomedical diagnostics, and environmental monitoring. They also advance high-performance, energy-efficient sensing technologies.

## 1.6 The Scope of the Study

The scope of this project encompasses the design and optimization of heterojunction-based FET devices for low-power sensing applications. The proposed system targets critical applications in industries such as environmental monitoring, healthcare, and industrial automation, where energy-efficient and high-performance sensors are essential. The project involves the use of advanced simulation tools, specifically TCAD software, to simulate and investigate the electrical and structural behavior of the proposed device. Through the optimization of device properties like as doping concentration and material choice, this research offers reliable and practical solutions for modern sensing challenges.

## 1.7 Limitation of the thesis

While the proposed HTFET biosensor designs show promise, their performance depends on several critical factors such as doping profiles, Accurate control over material properties, device geometry, and engineering is essential, as this influence tunneling efficiency, power consumption, and sensitivity.

Although SILVACO ATLAS provides valuable simulation capabilities, it may not fully capture real-world fabrication challenges and physical imperfections. Therefore, experimental validation is necessary to confirm the reliability and practical performance of the simulated designs.

## 1.8 Organization of the Thesis

This thesis is structured into five chapters, each serving a specific purpose. **Chapter 1** introduces the foundational concepts of MOSFETs, basic tunneling structures, Heterojunction Tunnel Field-Effect Transistors (HTFETs) and their relevance in low-power electronics, along with an overview of biosensors and their applications in modern sensing technologies. It also outlines the research problem, objectives, motivation, and scope of the study. **Chapter 2** provides a comprehensive literature review, analyzing prior work on HTFET architectures and biosensor integration to identify existing gaps and research opportunities. **Chapter 3** details the simulation methodology using SILVACO ATLAS TCAD, including device structures, material configurations, and modeling techniques. **Chapter 4** presents and interprets the simulation results, focusing on transfer characteristics, sensitivity analysis with different biomolecules, and the effects of dielectric engineering. Finally, **Chapter 5** summarizes the key findings, acknowledges limitations, and offers suggestions for future research in the development of advanced TFET-based biosensing devices.

# CHAPTER 2 LITERATURE REVIEW

## 2.1 Overview

This literature survey comprehensively reviews on Conventional MOSFEs, Tunnel Field-Effect Transistors (TFETs) and Heterojunction based TFETs, for low-power biosensing applications. It begins by outlining the fundamental principles of TFETs and their advantages over conventional Metal-Oxide-Semiconductor Field-Effect Transistors (MOSFETs) in addressing the fundamental power limitations of device scaling. The study then explores Heterojunction TFETs (HTFETs), emphasizing how bandgap engineering and architectural designs improve their performance. The use of TFETs and HTFETs in biosensing is covered in some detail, along with information on their high sensitivity, low power consumption, and compatibility with CMOS technology. Finally, the survey provides a comprehensive analysis of indium-based HTFET biosensors, discussing their unique material properties, highly advanced designs, and diverse applications, while also addressing associated fabrication challenges and future research directions.

## 2.2 Introduction to Tunnel Field-Effect Transistors (TFETs)

### 2.2.1 Evolution of Transistor Technology: Limitations of Conventional MOSFETs

The rapid miniaturization in semiconductor technology, largely governed by Moore's Law, has driven the evolution of integrated circuits. At the basic of these circuits are Metal-Oxide-Semiconductor Field-Effect Transistors (MOSFETs), which have served as the foundational electronic switches. However, as device dimensions continue to shrink, MOSFETs are encountering significant physical limitations that hinder further improvements in energy efficiency and performance. A primary constraint arises from their fundamental carrier transport mechanism, thermionic emission, which imposes a theoretical lower limit on the subthreshold swing (SS) of 60 mV/dec at room temperature (specifically, 63 mV/dec at 300. (Verreck et al., 2016) This inherent thermal limit restricts the extent to which the supply voltage (VDD) can be reduced without compromising the ON-state current, thereby limiting the achievable power savings. Beyond this fundamental SS limit, downscaling MOSFETs to nanoscale dimensions exacerbates a range of "short channel effects" (SCEs). These parasitic phenomena include Drain Induced Barrier Lowering (DIBL), where the drain voltage undesirably influences the channel potential, leading to a reduction in the threshold voltage (Vth) and increased OFF-state leakage current. Such effects contribute significantly to higher static power consumption, creating an inherent trade-off between the ON-current (ION) and OFF-current (IOFF) that fundamentally reduce the low-power performance of MOSFETs.

### 2.2.2 Fundamental Operating Principles of TFETs

The Tunnel Field-Effect Transistor (TFET) operates based on the principle of quantum mechanical band-to-band tunneling (BTBT), where charge carriers typically electrons tunnel across the bandgap from the valence band of the source to the conduction band of the channel. This tunneling is enabled by electric field-induced band alignment, which occurs under the influence of the gate voltage. Unlike conventional MOSFETs that rely on thermionic emission, where carriers must overcome a potential barrier, TFETs allow carriers to tunnel through the energy barrier, enabling sharper switching, operation at lower voltages, and a steeper subthreshold swing (SS) often below the theoretical 60 mV/decade limit of MOSFETs.

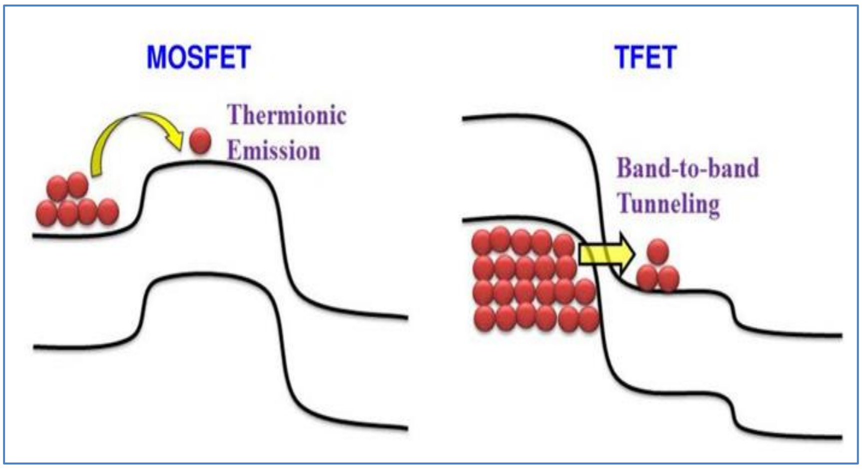


*Figure 2.1 Device principle of the MOSFETs and TFETs*

### 2.2.3 Transfer characteristics of TFET

The behavior of the device is described by the properties of the current that flow through it under various biased conditions. The transfer characteristics of a transistor are its most important properties. These typical transfer characteristics are graphs of the transistor's drain current with respect to the gate and drain bias ($I_D$-$V_{GS}$).

#### 2.2.3.1 OFF-State

In the OFF-state (VGS=0, VDS>0), charge carriers that are in the channel's conduction band are prone to drift to the drain region and generate a current. There aren't many electrons in the conduction band, though, because the source is p-type, so there aren't many electrons that can be injected into the channel. A small amount of OFF-state current is the outcome. An n-type source with a free electron in the conduction band is what happens in a MOSFET. The MOSFET based on thermionic emission will also inject a few of these electrons into the channel above the potential barrier at the source-channel junction. This results in a MOSFET having a higher OFF-state current than a TFET. (Datta et al., 2020)

#### 2.2.3.2 ON-State

Charge carriers must be introduced into the channel's conduction band in the ON-state (VGS>0, VDS>0) in order for current to flow through the device. Very few free electrons are created as charge carriers from the valance band of the source area in the conduction band of the p-type source region of TFETs. As the gate voltage (VGS) increases, the energy bands of the channel move relative to the source. The valance band in the source area and the conduction band in the channel align when the gate voltage is positive.

The electron in the source's valence band had no available energy state in the channel leading to the tunnel when the device was in its OFF state. The electron can now tunnel into the latter over the potential barrier created by the band-gap once the conduction band of the channel and the source's valence band have been identified. The source valance band and channel conduction band are arranged in this manner at the gate voltage, which marks the beginning of the TFET's ON-state (Karthik & Pandey, 2023).

#### 2.2.3.3 Ambipolar behavior

A positive gate voltage was applied when the drain voltage VDS was greater than zero. The channel's energy band travels upward to the source area when the gate voltage is lowered below 0V (VGS0). From the source valance band to the channel conduction band, no electron may tunnel when VGS=0. The number of states in the channel valence band that can be tunneled to the drain's conduction band grows as the negative gate bias increases, as does the tunneling length at the channel-drain junction. These factors combined result in a significant rise in drain current, a phenomenon known as ambipolar conduction. (Tiwari & Saha, 2022)

#### 2.2.3.4 Band Diagram

In MOSFETs, the current conduction mechanism is thermal carrier injection (over the barrier), while in TFETs, it is band-to-band tunneling (through the barrier). Electrons tunnel from the source valence band to the drain conduction band in an N-TFET (P-TFET, holes from the source conduction band to the drain valence band). The probability of BTBT is also impacted by changing the gate potential, which regulates the current. Because of the low source barrier in the ON state current (VGS>VDS>0V), thermionic carrier emission is possible. In the OFF-state current ($V_{GS}$=0V, $V_{DS}$>1 V), the source-side p-n junction barrier inhibits conduction in MOSFETs, restricting thermionic carrier emission. Due to the wide source to channel tunnel junction barrier (Low Electric Field), which results in very low OFF currents, the transmission probability of TFETs in the off state is low. Carriers are able to tunnel into the channel in the ON-state due to the tunnel barrier width. the BTBT generating process in TFETs increases subthreshold slope by less than 60mV/dec (Vimala et al., 2021).

#### 2.2.3.5 Work function

A fundamental property of solid material, which is a work function and defined as an energy required to remove electrons from the fermi level to the vacuum. It is typically measured in electron volts (eV) (Bergveld et al., 1998).

#### 2.2.3.6 Subthreshold slope

Subthreshold slope (SS) is a measure of how sleepy the drain current increase as the gate voltage is increasing in the subthreshold region. A subthreshold region is a range below the subthreshold voltage (Vt) where the transistor is fully turned on but still conducts some current. Whereas the subthreshold slope is measured in millivolts per decade (mV/Dec). The subthreshold slope (SS) is a critical parameter in the design of low-power circuits, as it dictates the minimum voltage necessary to maintain a desired level of current through the transistor. A smaller SS is highly desirable for low-power applications.

## 2.3 Heterojunction Tunnel Field-Effect Transistors (HTFETs)

Improved carrier mobility, reduced scattering effects, and adjustable energy band alignment to meet specific applications are only a few advantages of heterojunction materials, which are created by combining two semiconductors with different bandgaps.(Ghadimi Avval et al., 2018). Energy band alignment engineering is made possible by this feature, which greatly improves gadget performance.

Because they can achieve steeper subthreshold swings (SS) and higher ON-state current, heterojunction TFETs are a tempting alternative to traditional MOSFETs ((Hossain et al., 2024). In particular, these devices have shown an enhanced subthreshold swing as low as 16 mV/decade by employing a gate oxide overlapping approach, which significantly exceeds the conventional 60 mV/dec limit seen in conventional MOSFETs at ambient temperature. Because of their steep switching behavior and increased drive current, HTFETs are ideal for high-performance logic and ultra-low-power applications where speed and energy efficiency are crucial.

## 2.4 Related works

Biosensors are becoming more and more important for human health, with uses in security, environmental monitoring, and medicine (drug administration, early detection, and diagnosis). Through the processes of detection and transduction, these sensors transform the physicochemical reactions of biomolecules into measurable electrical impulses. Among various biosensor types, Field-Effect Transistor (FET)-based biosensors have garnered significant attention due to their advantages such as label-free detection, compact size, faster response, reliability, low cost, and capability for mass production (Swati et al., 2023).

Conventional diagnostic methods take a long time, cost a lot of money, and require sophisticated lab equipment, which can make them difficult to use quickly. On the other hand, biosensors based on Field-Effect Transistors (FETs) have emerged as a novel approach that can convert biological events straight into electrical signals. These biosensors are great candidates for portable and point-of-care diagnostic systems because of their many advantages, which include high sensitivity, label-free detection, low power requirements, scalability, and the potential for affordable, large-scale production (Theja & Panchore, 2023).

However, established FET-based biosensors, such as Ion Sensitive Field-Effect Transistors (ISFETs) and Metal-Oxide-Semiconductor FETs (MOSFETs), come with significant shortcomings. ISFETs are susceptible to signal drift and hysteresis, particularly under demanding conditions, whereas MOSFETs demand higher power and are restricted by a minimum subthreshold swing (SS) of 60 mV/dec at room temperature, falling short for ultra-low-power and highly scaled applications. Furthermore, FET biosensors face more general difficulties that can compromise their performance and scalability, such as integrating with Complementary Metal-Oxide-Semiconductor (CMOS) technology, the possibility of false positives or negatives, and issues with stability, selectivity, reproducibility, and Short Channel Effects (SCEs) (Swati et al., 2023).

The development and performance of biosensors that utilize Tunnel Field Effect Transistors (TFETs), marking a notable shift from traditional bio-sensing methods. Historically, the first biosensor was introduced in 1962, with Clark often recognized as the pioneer in this (Poorna Sundari & Lakshmi Priya, 2024).

Advanced FET topologies like Tunnel FETs (TFETs) have drawn more interest in an effort to overcome these difficulties. Specifically, vertical TFET-based biosensors (V-TFETs) show great promise for extremely selective and label-free biomolecule detection.

These biosensors are ideal for next-generation biomedical applications because they use vertical device topologies to enable greater electrostatic control, lower leakage currents, and ultra-low power consumption. ((Theja & Panchore, 2023).

The idea of charge plasma (CP) has been used to some of the TFET's shortcomings. By employing appropriate electrode work functions, this method does away with the requirement for doping in the source and drain regions. This method produces charge plasma TFET-based devices that are easier to build, have a reduced thermal budget, and are less vulnerable to random dopant variations and device variability(Swati et al., 2023).

To overcome issues with high leakage current and low sensitivity in TFETs, negative capacitance TFET-based biosensors (NCTFET) are being investigated. Reduced IOFF, better ION/OFF, reduced power consumption, and higher performance are all provided by NCTFETs. Comparative studies reveal that NCTFETs perform better than conventional TFETs in terms of low IOFF and SS avg, ION/IOFF ratio, and sensitivity. ((Poorna Sundari & Lakshmi Priya, 2024)

Additionally, TFET biosensors are made to identify particular cancer biomarkers. Using the unique dielectric properties of healthy and malignant cells, a novel dielectric modulated dopingless dual metal gate heterojunction TFET (DM-DL-DMG-HJTFET) is presented for label-free detection of breast cancer cell lines. For T-47D cells, this design demonstrated exceptional sensitivity. (Dewan et al., 2024).

Heterojunction TFET-based biosensors regulate the tunneling by using flexible bandgap materials at the source-channel interface. To increase performance, materials such as SiGe, AlGaAsSb, InGaAs, and InSb are utilized. The DC-HJ-TFET biosensor is highlighted for its remarkable sensitivity, favorable ION value, and excellent ION/IOFF ratio (Poorna Sundari & Lakshmi Priya, 2024).Heterojunction TFETs can have their tunneling width reduced and their drain current improved by using a smaller bandgap material, such as GaSb, in the source region.

Advanced electronic and optoelectronic devices, such as high-performance HTFET biosensors, have great potential thanks to indium-based semiconductor materials, especially indium phosphorus (InP) and indium gallium arsenide (InGaAs). Their primary advantage is that they have tunable and direct bandgaps, which are necessary to increase the band-to-band tunneling (BTBT) likelihood and, hence, the ON-current in TFETs. InP, for instance, is highly valued for its high carrier mobility, which makes it crucial for high-speed operations.

This makes it essential for high-frequency and high-speed optoelectronic devices like modulators, lasers, and photodetectors. Miniaturized, high-efficiency components benefit greatly from its exceptional electron mobility and frequency capabilities. Even with these better electrical qualities, there are still significant obstacles to the broad use of indium-based materials in biosensing applications. (Saravanan et al., 2022).

The main purpose of using indium antimonide (InSb) as the source material is to increase the ON current. InSb was chosen due to its low effective mass, greater carrier mobility, and lower energy gap of about 0.17 eV. The Band-To-Band Tunnelling (BTBT) rate is increased by InSb's lower tunneling barrier when compared to silicon and germanium. The suggested InSb/Si TFET greatly increases the ON current by reducing the channel length at the source-channel interface by employing silicon for the channel and drain and InSb for the source side (Kumar & Sivani, 2016).

Biomolecules inside the TFET cavities result in efficient coupling at the tunnel side, which raises sensitivity. TFET technology's intrinsic low-power properties enable sophisticated biosensing applications. Drain current sensitivity (Sn), which is the ratio of drain current with biomolecules (Ibio) to that with air (Iair), is a crucial performance metric for biosensors. (Kumar & Sivani, 2016)). Higher sensitivity indicates better performance. Various studies have reported different sensitivity parameters, including drain current sensitivity and transconductance sensitivity. The drain current is also influenced by the fill factor, which indicates the percentage of the nanocavity that is filled with biomolecules. (Kumar & Sivani, 2016).

When the dielectric constant of the biomolecules inside the cavity region rises, the effective gate capacitance also rises because of the enhanced border fields. A larger dielectric constant results in a higher potential beneath the oxide-silicon interface, a higher gate capacitance, and a lower potential drop across it. By causing a downward shift in the energy band diagram, this enhanced potential lowers the tunneling barrier width and increases the likelihood of tunneling. (Theja & Panchore, 2023).

DMG-SS-BTFET is a new Dual Metal Gate-Split Source-Bilateral TFET that is intended for high-frequency and ultra-low-power applications. Its highly doped germanium F-shaped split-source arrangement, which incorporates a dual-metal gate and a $n^+$ pocket to improve tunneling at the source/pocket (S/P) interface, is the main innovation. Because of the source's location within the channel, this architecture allows for several tunneling pathways, including point, line, and diagonal, hence expanding the tunneling area and enhancing ON-state performance. The proposed DMG-SS-BTFET showed a significantly lower subthreshold swing (2.25 mV/dec) compared to a conventional DMG-BTFET (16.8 mV/dec), and achieved a high ION/IOFF ratio of $1.72 \times 10^{12}$. (Hamza et al., 2112).

In conclusion, the strategic combination of TFET's quantum tunneling mechanism with heterojunction engineering and advanced architectural designs positions these devices as leading candidates for next-generation low-power biosensing applications. Continued research into novel materials, fabrication techniques, and comprehensive optimization strategies will be essential to overcome existing challenges and unlock the full potential of heterojunction-based TFETs for widespread impact in healthcare, environmental monitoring, and beyond.

*Table 2.1 Summery of different TFET Biosensor*

| Author | Title | Performance | Limitations |
|---|---|---|---|
| (Theja & Panchore, 2023) | Performance Investigation of GaSb/Si Heterojunction Based Gate | Subthreshold swing <60 mV/dec, low power consumption, high sensitivity (transconductance | Selectivity issues, scaling difficulties |

| | | | |
|---|---|---|---|
| | Underlap and Overlap Vertical TFET Biosensor | sensitivity: $5.8 \times 10^5$, drain current sensitivity: $5.6 \times 10^5$ | |
| Sukanta (Kumar & Sivani, 2016) (Swain et al., 2021), (Swain et al., 2021) | InSb/Si Heterojunction-Based Tunnelling Field-Effect Transistor with Enhanced Drive Current and Steep Switching | Subthreshold swing: 50 mV/dec, max cut-off frequency: 777.8 GHz, GBW: 393 GH | Complexity of device structure, integration challenges |
| (Poorna Sundari & Lakshmi Priya, 2024) | Nano-biosensors with subthreshold swing tunnel field effect transistor: A cutting-edge review | Subthreshold swing <60mv/Dec, low power consumption, high sensitivity | Selectivity issues, scaling difficulties |
| (Ahish et al., 2016), (Ahish et al., 2017),(Kumar & Sivani, 2016) | Prospects and challenges of sensor materials: A comprehensive review | Transformation of stimuli into quantifiable signals, enhanced performance with nanomaterials | Response speed, selectivity, sensitivity, durability, cost-effectiveness |
| (Hossain et al., 2024) | InSb/Si Heterojunction-Based Tunnelling Field-Effect Transistor with Enhanced Drive | I_ON/I_OFF ratio: $\sim 10^{12}$, Average subthreshold swing: 29 mV/decade | Potential fabrication challenges with InSb, cost implications |

| | | | |
|---|---|---|---|
| | Current and Steep Switching | | |
| (Saravanan et al., 2022) | Analysis of InAs-GaAs Gate-all-around Tunnel Field Effect Transistors (GAA-TFET) | low off-current (IOFF) of 2.27 x 10-17 A/m, a high enhanced ION of 7.39 x 10-6 A/m, sub-threshold swing (SS) was 16.8 mV/dec. | Complex fabrication, |
| (Bhattacharyya et al., 2019), Debashis De (2020) | Performance Assessment of New Dual-Pocket Vertical Heterostructure Tunnel FET-Based Biosensor Considering Steric Hindrance Issue | - Comprehensive sensitivity evaluation across physical design variables.<br><br>- High sensitivity and linearity even with irregular biomolecule | - lacks experimental validation.<br>- Device complexity due to dual-pocket and heterostructure design.<br>- Effects like process variability and thermal noise not considered. |

# CHAPTER 3 METHODOLOGY AND STRUCTURE DESCRIPTION

## 3.1 Frame of the Research

To achieve the general and specific objectives of this study, a systematic methodology was followed, as outlined in the flowchart. The process commenced with a comprehensive literature review to gain insight into existing FET and TFET-based biosensors. This enabled the identification of research gaps, which guided the analysis of advanced device structures. A novel biosensor model was then simulated using TCAD tools to evaluate its electrical and biosensing performance. The resulting data were analyzed and compared with existing studies to assess improvements in sensitivity, ON/OFF current ratio, and overall device efficiency, thereby validating the proposed design.

.

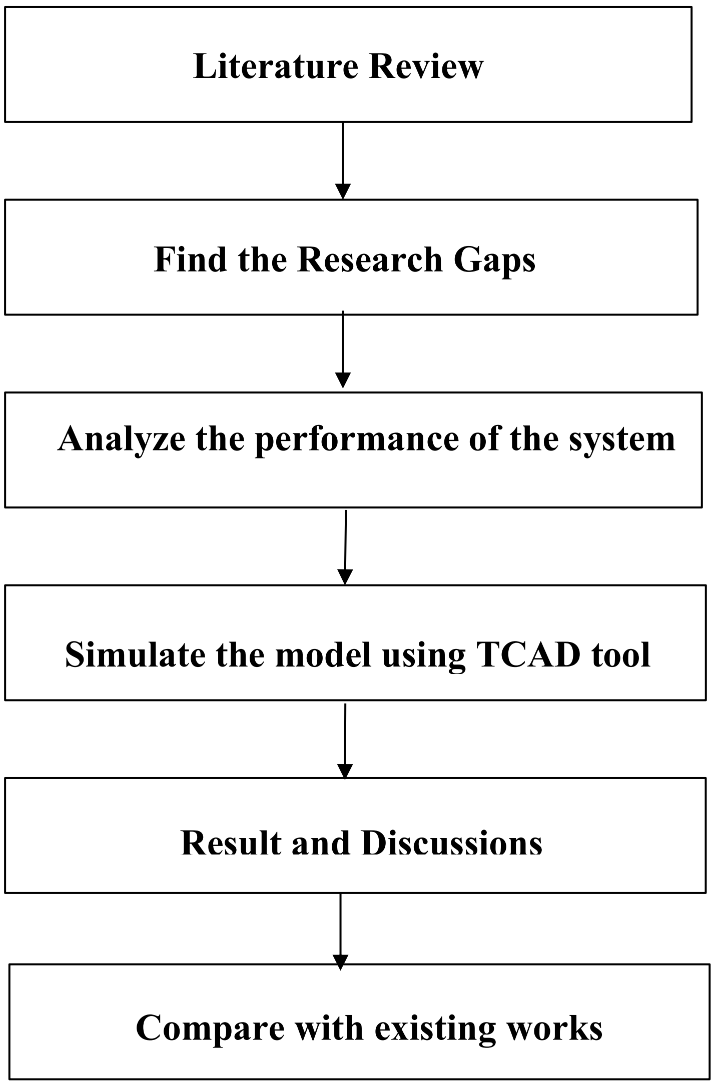


*Figure 3.1 Frame Work of the research*

## 3.2 Material requirement (Software)

**Silvaco Atlas TCAD (version 5.0.10.R**): This is a comprehensive suite of software tools used for simulating and modeling semiconductor devices and processes. It enables engineers to visualize internal physical processes, optimize device designs, and reduce development costs and time-to market. It is the primary software we used to model and simulate the performance of the device being investigated. It probably employs a digital representation of the device to predict how it would operate in a real-world setting.

**Origin:** This tool is crafted to facilitate the analysis and visualization of data, likely by importing simulation results from Silvaco Atlas, allowing users to create graphs and charts that improve understanding of the data.

**PowerPoint:** This application is utilized for generating schematics and illustrations. It is probably employed to depict the physical layout of the simulated device and potentially flowcharts to outline the simulation procedure. Our workflow involved utilizing Silvaco Atlas for conducting virtual experiments on the device, Origin for result analysis, and PowerPoint for creating visual representations of the device and simulation process.

### 3.2.1 Silvaco TCAD Atlas Tools

The proposed device simulation will be conducted using Silvaco Atlas TCAD simulation software, a powerful tool developed by Silvaco, a company founded in 1984 and based in (Santa Clara, 2004)alifornia. Renowned for its advanced Computer-Aided Design (CAD) simulation tools, Silvaco supports a wide range of semiconductor technologies, catering to both industrial and research applications.

Silvaco's Atlas software enables comprehensive, physically based simulations for semiconductor devices in both two-dimensional (2D) and three-dimensional (3D) configurations. To enhance the simulation process, the Atlas suite integrates with Virtual Wafer Fabrication (VWF) Interactive Tools, including Mask Views, Optimizer, Deck Build, Tony Plot. These tools extend the software's functionality, enabling researchers and developers to accurately replicate semiconductor devices for research and development.

By closely mirroring the experimental characteristics of devices, these tools provide valuable insights into the behavior and performance of emerging semiconductor technologies. Moreover, they are instrumental in predicting the full spectrum of features and attributes of new devices and processes, making them a key asset for advancing semiconductor research and development.

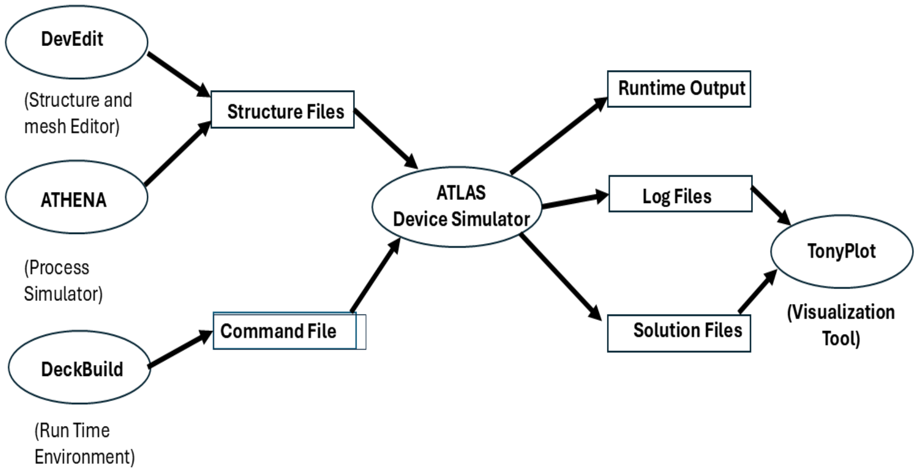


*Figure 3.2 Atlas input and output*

## 3.3 Design Methodology

### 3.3.1 Simulation Procedures and Devices

As shown in Figure 3.2, the device structures simulated in this work, such as the InAs device with an InGaAs source pocket and the proposed Ge split-source HTFET, were created using the previously mentioned simulation processes, starting with mesh definition and ending with visualization plots.

### 3.3.2 Structure Specification

This step involves specifying the mesh, regions, materials, electrodes, and doping profiles in the input file, using the MESH, REGION, ELECTRODE, and DOPING statement.

*Table 3.1 ATLAS command categories and their main statements*

| Group | Statements |
|---|---|
| 1. Structure Specification | mesh, region, electrode, doping |
| 2. Material Models Specification | material, models, contact, interface |
| 3. Numerical Method Selection | method |
| 4. Solution Specification | log, solve, load, sav |

| | |
|---|---|
| 5. Results Analysis | extract, tonyplot |

**A) Meshing**

It is a very critical part of the design; it defines the device structure in 2-D in Cartesian grid. The x-axis side mesh (X. mesh) occur on the left to the right and y-axis mesh (Y. mesh) is from bottom to top (Santa Clara, 2004)

**B) Regions**

Region is the statement, which separate the initial mesh into blocks and the material parameters; each block is given its own region number. In region definition the area the mesh location should be specified from the lowest to highest (Santa Clara, 2004)

**C) Electrode**

An electrode refers to a terminal or contact region of a semiconductor device where voltage is applied or current is collected and electrode positions defined within the mesh. Electrodes play a key role in defining the electrical boundary conditions for simulation

**D) Doping**

The doping statement defines doping profiles within the device structure, either through analytical methods or by using data from an input file. The syntax is as follow below:

DOPING <distribution type> <dopant type> <position parameters>

### 3.3.3 Material

This statement assigns a physical parameter to the mesh. It is necessary to connect the previously identified doped region with particular materials. The Atlas has already established material and parameters, which are crucial for the semiconductor and do not need to be altered.

E.g. material= silicon, material=InSb

### 3.3.4 Simulation models

In semiconductor device design and modeling, a variety of physical models are employed to accurately simulate carrier transport, generation, and recombination mechanisms. Among them, models such as AUGER, FLDMOB, BQB, NON-LOCAL BTBT, Shockley-Read-Hall

(SRH), and CONMOB play crucial roles in advanced device simulations (Santa Clara, 2004)

In our simulation framework, NON-LOCAL BTBT and LOCAL BTBT models were used to describe band-to-band tunneling, a key mechanism in devices like TFETs. These models account for carrier generation due to tunneling across the bandgap. While the LOCAL BTBT model calculates the generation rate based on the electric field at each mesh node, it assumes the tunneling process is localized. In contrast, the NON-LOCAL BTBT model accounts for the spatial distribution of the energy bands, more accurately capturing the tunneling phenomenon by considering the non-local nature of the process and the spatial separation of generated carriers.

The FLDMOB model is used to simulate low electric field-dependent carrier mobility, whereas CONMOB incorporates the effects of high electric fields on mobility behavior. These mobility models allow for accurate concentration- and field-dependent mobility calculations.

The BQB (Band-to-Band Generation by Tunneling) model is another tunneling model that describes the movement of charge carriers across the bandgap due to quantum tunneling effects.

For recombination mechanisms, the Shockley-Read-Hall (SRH) model is used to estimate carrier recombination rates through trap states, while the AUGER model explains impact ionization, where energetic carriers generate additional electron-hole pairs, contributing to increased current flow. Together, these models enable comprehensive and precise simulation of semiconductor devices such as TFETs, improving understanding and aiding in design optimization. E.g. models cvt conmob fldmob srh fermi ni. fermi bgn auger bbt. nonlocal

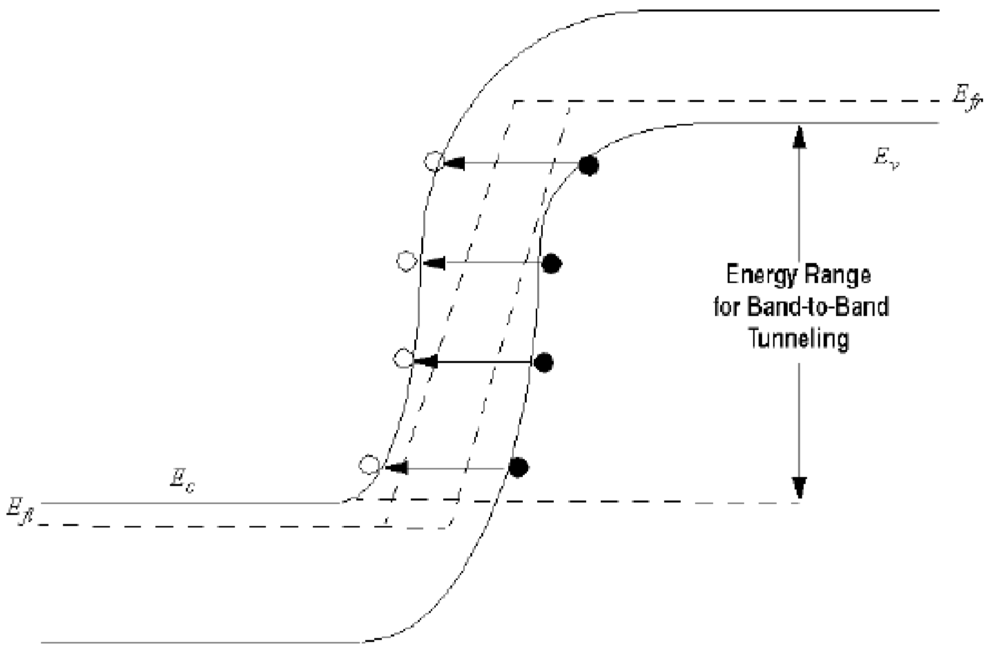


*Figure 3.3 Diagram of reverse bias non-local band-to-band tunnelling*

ATLAS computes the spatial start and end positions for the tunnelling at each energy, E, which we designate $X_{beg}$ and $X_{end}$. It does this by considering each energy within the permitted range. For an electron in the energy range E - ΔE/2 to E + ΔE/2 (where ΔE is a tiny energy increment), the contribution to tunnelling current is

$$J(E) = \frac{qKTm^*}{2\pi^2\hbar^3} T(E) \ln \left\{ \frac{1 + \exp\left[\frac{E_{fl} - E}{kT}\right]}{1 + \exp\left[\frac{E_{fr} - E}{kT}\right]} \right\}$$

$$\Delta Em *= m_0 \sqrt{\left(m_e(x_{end}) * m_h(x_{beg})\right)}$$

If $E_{fl} < E_{fr}$, the current has a negative sign; otherwise, it has a positive sign. As expected, there is no current when there is equilibrium, as $E_{fl} = E_{fr}$.

### 3.3.5 Solution method

The METHOD statement in TCAD defines the numerical techniques used to solve physical equations and associated parameters (Santa Clara, 2004). Although the ATLAS library offers several numerical approaches, three main methods are commonly used. The GUMMEL method is suitable for weakly coupled systems and provides linear convergence with relatively low computational effort. In contrast, the NEWTON method is more appropriate for tightly coupled systems, offering quadratic convergence and higher accuracy but requiring more computational time and a precise initial guess to ensure stability. When the Newton method fails to converge reliably, the BLOCK method can be used to accelerate simulations, albeit with a trade-off in precision. In our simulations for both proposed devices, we adopted the NEWTON-TRAP method, as it provides robust convergence and accurately captures trap-assisted phenomena in complex device structures**.**

### 3.3.6 Specification of solutions

For creating data, files in Atlas Simulator solve/log/save instructions are used. Those instructions (solve/log/save) work together to analyses and generate data. To analyses the device structure these statements are used drain current with respect to gate voltage (Santa Clara, 2004)

### 3.3.7 Extracting and plotting data

The final part of the input deck involves data extraction and visualization using the **EXTRACT** statement in DeckBuild. This flexible, case-sensitive command allows users to define custom extraction algorithms and retrieve device parameters from solved curve or structure files. For visualization, the output log files must be saved and loaded into **TONYPLOT**, where electrical characteristics such as current-voltage behavior can be plotted and analyzed.

## 3.4 Device structures

### 3.4.1 Source-Engineered Heterojunction TFET

The Source engineered TFET involves modifying the source region to optimize band-to-band tunneling (BTBT), which is the primary mechanism for current flow in TFETs. Unlike traditional MOSFETs, TFETs operate by tunneling electrons from the valence band of the source to the conduction band of the channel, which helps to get a steep subthreshold swing (below the 60 mV/decade limit of MOSFETs) to make the optimize low-power operation. Source engineered is term when we introduce some device level technique in tunnel FET to make it suitable for high-speed applications. Following measures can be taken to optimize the source for better performance.

1. **Material Selection:** Materials with a smaller bandgap or favorable band alignment are chosen to reduce the tunneling barrier and enhance device performance. The materials

used in this work, along with their corresponding bandgaps and effective masses, are listed in the following *table 3.2*.

*Table 3.2 Heterojunction Materials used in the work*

| Materials | Energy bandgap(eV) | Electron Effective Mass($m*/m_o$) | Hole Effective Mass ($m*/m_o$) |
|---|---|---|---|
| InAs | 0.35 eV | ~0.023 | ~0.41 |
| InSb | 0.17eV | ~0.013 | ~0.4 |
| InGaAs | 0.35 eV (indium arsenide) to 1.42 eV (gallium arsenide) | ~0.041 | ~0.45 |
| InP | 1.344 eV | ~0.08 | ~0.6 |
| Ge | 0.67eV | ~0.12 | ~0.3–0.34 |

**2.Structural Modifications**: Introducing features like a split source or a pocket region to sharpen the electric field and enhance tunneling probability.

**3.Doping Profiles**: Heavily doping the source (e.g., p-type at $1\times10^{20}$ $cm^{-3}$,) to increase carrier availability for tunneling

### 3.4.2 Source-Extended Heterostructure TFET with Indium-Based Drain

#### 3.4.2.1 Conventional TFET and InP_Drain_ HTFET

As shown in the *figure 3.4* below the conventional Tunnel Field-Effect Transistor is designed with a hafnium dioxide ($HfO_2$) gate stack for improved insulation and control. Its structure consists of a heavily p-type doped silicon source at $1\times10^{20}$ $cm^{-3}$, a moderately n-type doped silicon channel at $1\times10^{17}$ $cm^{-3}$, and a heavily n-type doped silicon drain at $1\times10^{19}$ $cm^{-3}$. This all-silicon configuration ensures a uniform material system throughout the device.

In contrast, the Silicon-Indium Phosphide (Si/InP) TFET in figure 3.5 shares the same silicon source and channel, with doping concentrations of $1\times10^{20}$ $cm^{-3}$ (p-type) and $1\times10^{17}$ $cm^{-3}$ (n-type), respectively. However, it features a heavily n-type doped indium phosphide (InP) drain at $1\times10^{20}$ $cm^{-3}$, forming a heterojunction at the channel-drain interface.

The detailed structures of both the Si/Si TFET and the Si/InP TFET are illustrated in *the figures 3.4 and 3.5* below. A comprehensive analysis of their transfer characteristics and performance metrics will be provided in the following chapter.

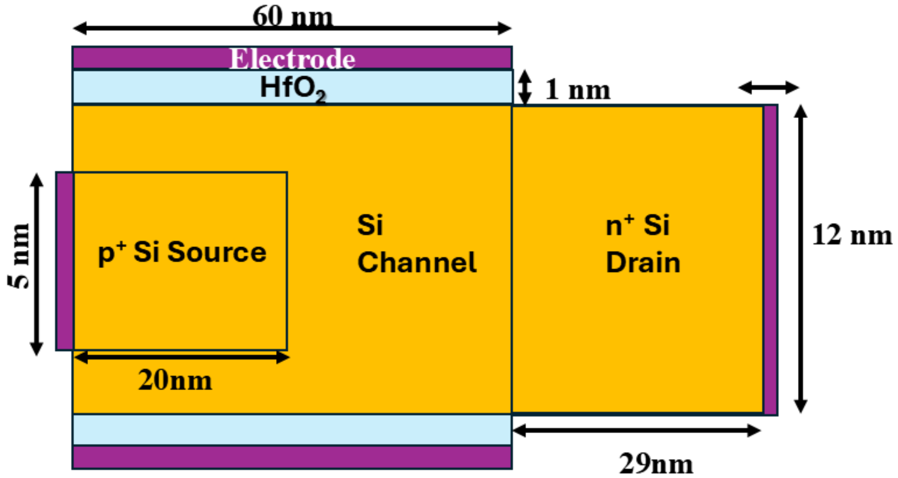


*Figure 3.4 Conventional TFET Structure*

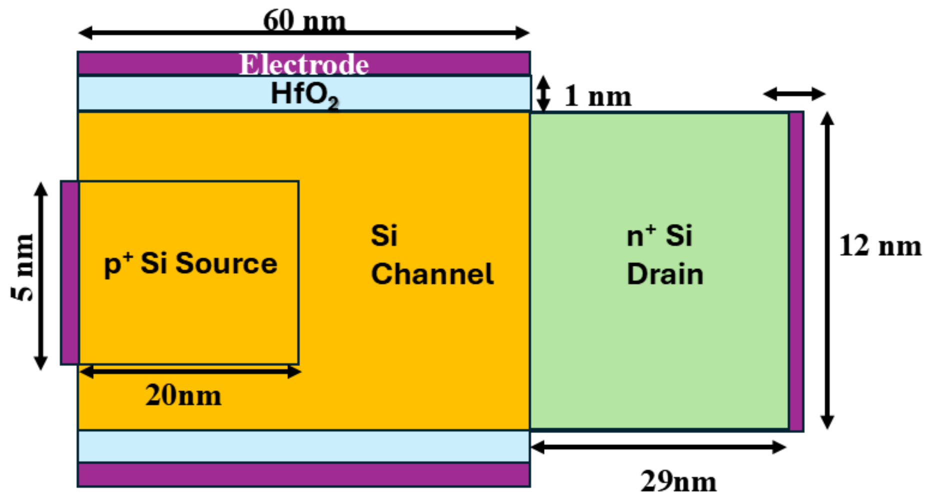


*Figure 3.5 Structure of InP_Drain_ HTFET*

#### 3.4.2.2 Ge/InSb-Source- Si -drain HTFET

The double gate heterojunction TFET features a gate oxide of hafnium dioxide ($HfO_2$) in *figure 3.6*, which provides excellent insulation and enables precise dual-gate control. Its structure consists of a heavily p-type doped InSb source at $1\times10^{20}$ $cm^{-3}$, a moderately n-type doped silicon channel at $1\times10^{16}$ $cm^{-3}$, and a heavily n-type doped silicon drain at $1\times10^{19}$ $cm^{-3}$.

In contrast, the Ge- source HTFET in *figure 3.7* shares the same source and channel, with doping concentrations of $1\times10^{20}$ $cm^{-3}$ (p-type) and $1\times10^{16}$ $cm^{-3}$ (n-type), respectively, and a heavily n-type doped silicon drain at $1\times10^{19}$ $cm^{-3}$.

The detailed structures of both TFETs are shown in the figures below for better understanding, and a comprehensive analysis of their transfer characteristics will be presented in the next chapter.

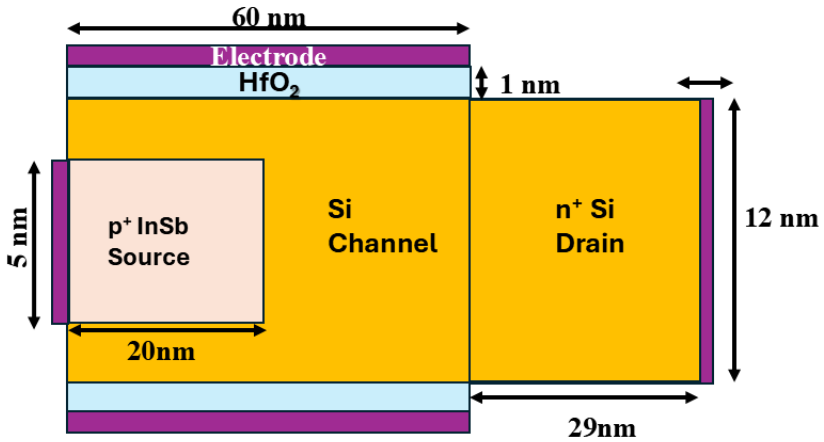


*Figure 3.6 InSb-Silicon HTFET Structure*

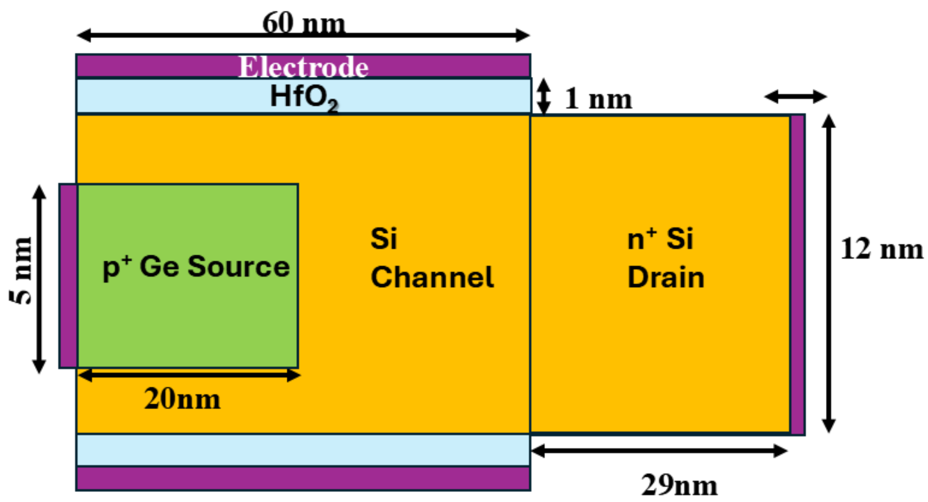


*Figure 3.7 Structure of Ge-Silicon HTFET*

#### 3.4.2.3 Ge/InSb-Source- InP -drain HTFET

As shown in Figure *3.8 and Figure 3.9* both the Ge/InP and InSb/InP HTFETs are engineered as double-gate heterojunction devices, with a gate oxide constructed from hafnium dioxide ($HfO_2$). A comprehensive log file comparison, to be explored in the next chapter, is anticipated to provide empirical validation of these performance differences.

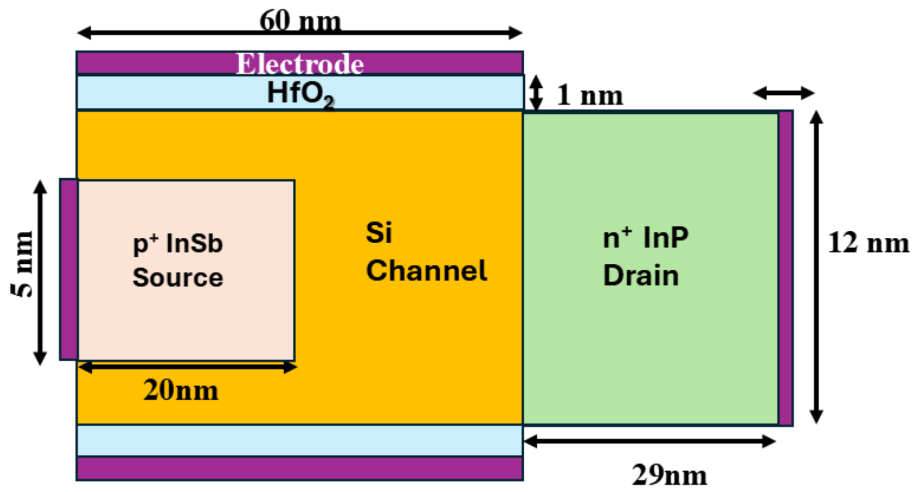


*Figure 3.8 InSb-Source- InP HTFET Structure*

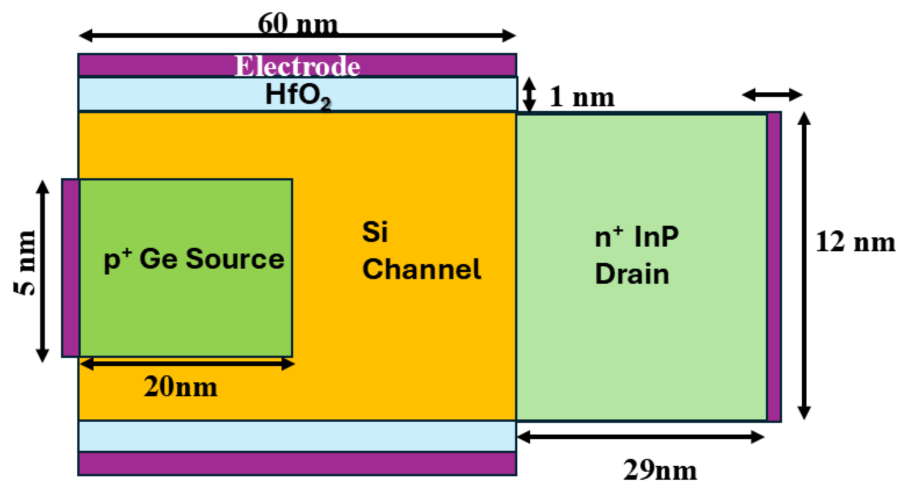


*Figure 3.9 Structure of Ge--Source -InP HTFET*

#### 3.4.2.4 Germanium Split Source extended Heterostructure TFET

The Ge-split-source or F-shaped source configuration, HTFETs are advanced double-gate heterojunction tunnel field-effect transistors (TFETs) featuring identical gate oxide with high-k hafnium dioxide ($HfO_2$) as the gate dielectric. This device variants employ uniform doping profiles, including a heavily p-doped germanium (Ge) source at $1\times10^{20}$ cm$^{-3}$, a heavily n-doped indium phosphide (InP) drains at $1\times10^{20}$ cm$^{-3}$, and a moderately n-doped silicon channel.

We found this device to be well-suited for biosensor design due to its superior performance characteristics, including higher ON-current, improved subthreshold swing, lower leakage current, and enhanced ambipolar current suppression an essential parameter for achieving efficient low-power biosensing. The proposed design utilizes a split-source, or F-shaped source configuration, which combines highly doped germanium (Ge) material with electric field crowding effects. This design enables a combination of point, line, and diagonal tunneling mechanisms, which collectively enhance the ON-state current of and significantly reduce the subthreshold swing.

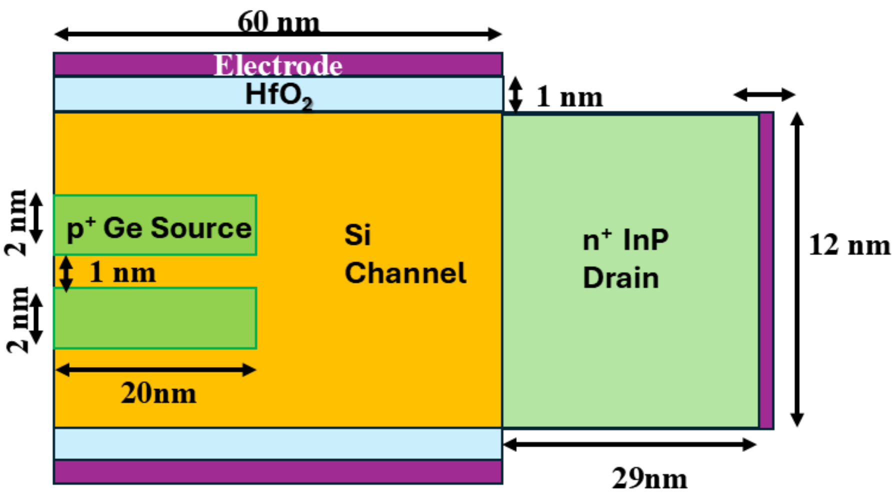


*Figure 3.10 Structure of Ge- Split-Source -HTFET*

This chapter discusses various TFET device structures with a focus on source engineering. The structures explored include the Conventional TFET, InP_Drain_HTFET, InSb-Source/InP HTFET, Ge-Source/InP HTFET, Ge-Silicon HTFET, Ge-Split-Source HTFET, and InSb-Silicon HTFET. Finally, the chapter presents the novel structure proposed for the biosensor application.

The proposed biosensor, shown in *Figure 3.11*, features the same source, drain, and channel material concentrations as previous structures shown in *figure 3.10*, with the addition of a heavily doped silicon pocket in the source region at a concentration of $1\times10^{19}$ cm$^{-3}$. This modification is designed to enhance tunneling probability, reduce leakage current, and improve overall switching performance, making the device well-suited for low-power, high-efficiency applications.

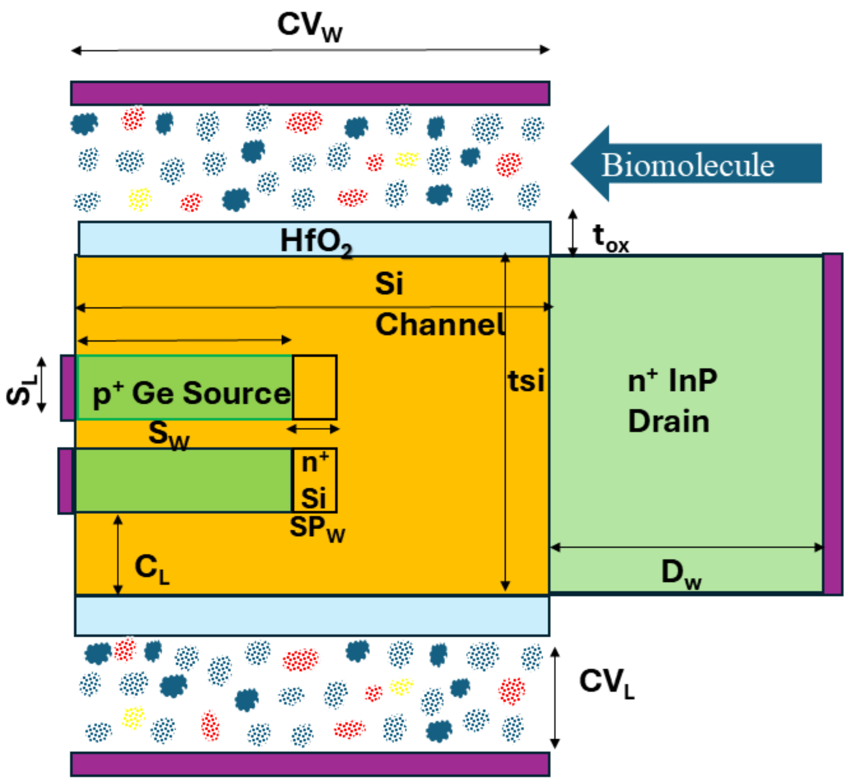


*Figure 3.11 Device Structure of Ge- Split-Source -HTFET Biosensor*

*Table 3.3 Parameters used for simulation of the proposed Biosensor*

| Parameters | Proposed Ge- Split-Source -HTFET Biosensor |
|---|---|
| Source concentration (Na) (cm-3) | $1\times10^{20}$ |
| Channel concentration (Nd) (cm-3) | $1\times10^{16}$ |
| Drain concentration (Nd) (cm-3) | $1\times10^{19}$ |
| Channel thickness (nm) | 60 |
| Cavity Width(nm) | 60 |
| Cavity Length(nm) | 3 |

| | |
|---|---|
| Source length (nm) | 4 |
| Drain length (nm) | 12 |
| Channel length (nm) | 12 |
| N+ Si Source pocket concentration (cm-3) | $1\times10^{19}$ |
| N+ Si Source pocket width(nm) | 10 |
| N+ Si Source pocket length (nm) | 4 |
| Thickness of $HfO_2$ (nm) | 1 |

## 3.5 Overview of Horizontal Heterojunction TFET(HTFET)

### 3.5.1 Engineering Modifications in Conventional TFET Design

TFETs suffer from certain performance limitations that hinder their widespread adoption. The most notable challenges include:

- Low ON-state current (ION), which arises from the inherently limited tunneling probability compared to thermionic emission in MOSFETs.
- Ambipolar conduction, a phenomenon where undesirable reverse-bias tunneling occurs at the drain-channel junction, leading to increased OFF-state current and reduced device reliability.

To address these limitations and push TFETs closer to practical deployment, this work explores the impact of several strategic structural and material design modifications. Specifically, the study investigates:

1. **Advanced III-V Material System** – Indium Arsenide (InAs) is used as the source material, while Indium Phosphide (InP) is employed for both the channel and drain regions. InAs, with its low effective mass and narrow bandgap, facilitates efficient band-to-band tunneling. InP, on the other hand, offers superior lattice matching and thermal stability.

This material combination enables the formation of staggered or broken-gap heterojunctions, which enhance tunneling efficiency while maintaining robust control over short-channel effects.

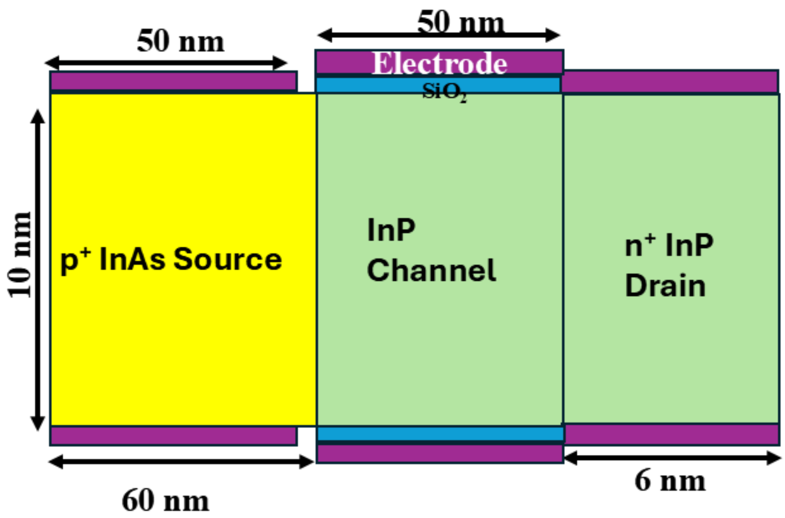


2.

*Figure 3.12 InAs/InP HTFET Structure*

3. **Dielectric Pocket Integration** – The introduction of a dielectric pocket near the drain side using hafnium dioxide ($HfO_2$), a high-k dielectric. This modification aims to suppress ambipolar conduction by increasing the tunneling barrier width at the drain-channel interface, effectively reducing leakage current during the OFF state.

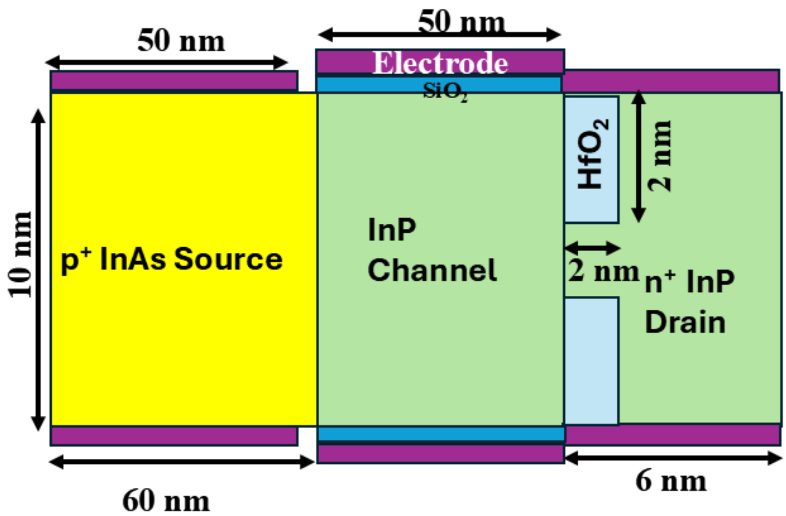


*Figure 3.13 InAs/InP with Dielectric Pocket (DP) Structure*

4. **Source Pocket Engineering** – The incorporation of a source pocket region near the source-channel interface, doped with Indium Antimonide (InSb), a material known for its extremely narrow bandgap and high electron mobility. This region is expected to enhance the tunneling rate and significantly boost the ON-state current by steepening the band profile at the tunneling junction.

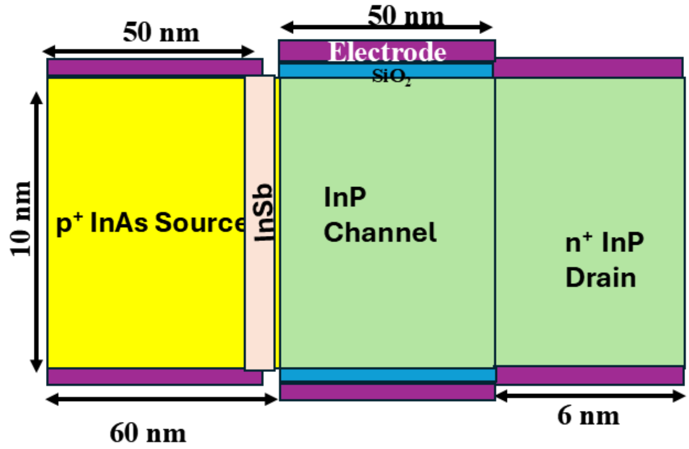


*Figure 3.14 InAs/InP with Source Pocket (SP) Structure*

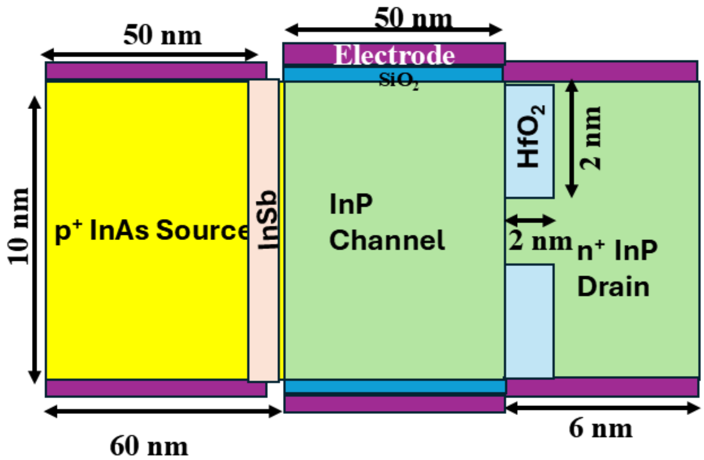


*Figure 3.15 InAs/InP with Source and Dielectric Pocket Structure*

## 3.6 Fundamentals of Vertical Heterojunction TFET Architecture

At the beginning of this chapter, we discussed the source-extended structure, a variation of vertical TFETs designed to enhance tunneling efficiency. In addition to this, we also designed a vertical Heterojunction Tunnel Field-Effect Transistor (V-HTFET) featuring an InAs source combined with a SiGe pocket. As previously discussed, InAs possesses a lower bandgap and effective mass. This greatly improves tunneling efficiency, which makes it ideal for TFET operation. Table 3.5 lists the design specifications for this device structure.

Table 3.4 Parameters used for simulation for the vertical device structure

| Parameters | Proposed InAs with InGaAs Pocket Biosensor |
| --- | --- |
| Source concentration (Na) (cm-3) | $5\times10^{19}$ |
| Channel concentration (Nd) (cm-3) | $1\times10^{12}$ |
| Drain concentration (Nd) (cm-3) | $5\times10^{18}$ |
| Channel thickness (nm) | 10 |
| Source length (nm) | 15 |
| Drain length (nm) | 20 |
| Channel length (nm) | 37 |
| N+ pocket concentration (cm-3) | $5\times10^{19}$ |
| N+ pocket length (nm) | 5 |
| Thickness of $SiO_2$ (nm) | 1 |
| Thickness of $HfO_2$ (nm) | 6 |

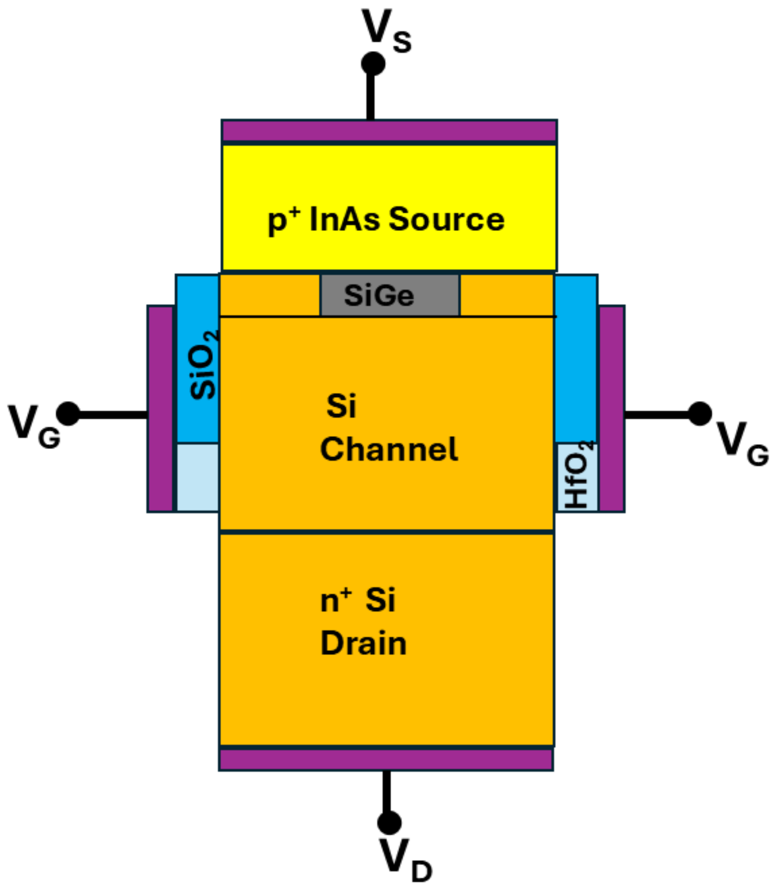


*Figure 3.16 Device Structure Silicon with SiGe Pocket V-HTFET*

Heterojunction TFET-based biosensors utilize bandgap-engineered materials at the source-channel interface to effectively control the tunneling rate. Materials such as AlGaAsSb, InGaAs, and InSb are employed to enhance device performance by facilitating efficient carrier transport. Incorporating a low bandgap material like InAs in the source region reduces the tunneling barrier width, thereby increasing the drain current and enabling designs with an excellent ION/IOFF ratio an essential feature for high-performance, low-power biosensing applications. (Poorna Sundari & Lakshmi Priya, 2024).

Based on the above considerations, InGaAs was found to be a suitable material for the source-channel pocket in enhancing vertical HTFET performance. Its favorable band alignment and moderate bandgap made it ideal for improving tunneling efficiency, thereby supporting the development of low-power, high-performance biosensing devices.

The proposed biosensor device features a source doping concentration of $5\times10^{19}$ source concentration, a drain concentration of $5\times10^{18}$ drain concentration and a channel concentration of $1\times10^{12}$.It incorporates a highly doped InGaAs region with a concentration of $5\times10^{19.}$

Additionally, the device includes a sensing cavity with a length of 15 nm and a width of 5 nm, optimized for enhanced sensitivity and tunneling efficiency in low-power biosensing applications.

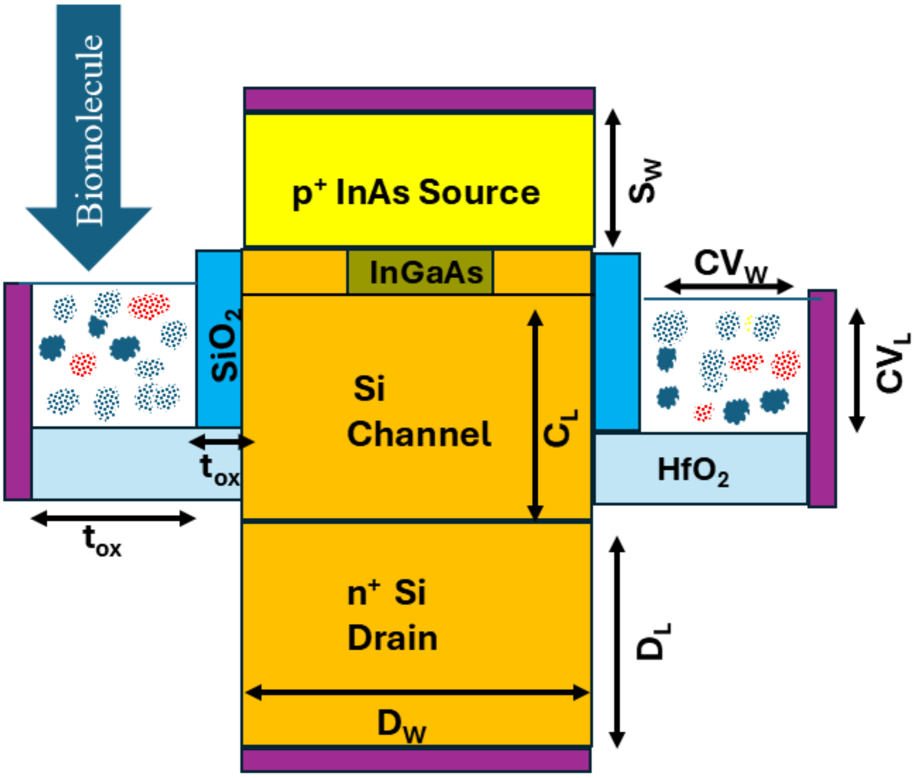


*Figure 3.17 Proposed structure of InAs with InGaAs pocket Biosensor*

# CHAPTER 4 RESULT AND DISCUSSION

In this chapter, we compared the simulated structures and investigated the performance of the proposed design for low-power and high-speed applications. To determine the optimized structure, we replaced the source and drain materials and also examined horizontal, vertical, and source-extended TFET configurations. From an application perspective, we utilized both types of structures to develop low-power FET-based biosensors. The biosensors analyzed in this work were based on two distinct architectures: the Ge split-source HTFET and the vertical heterojunction TFET. Based on the results, it was observed that the biosensor incorporating the vertical HTFET architecture performed better than the Ge split-source-based design, primarily due to the greater ON-current variation observed when modulating the dielectric properties of biomolecules in the gate region.

## 4.1 Impact of Indium phosphide (InP) In source Extended HTFET

As illustrated in *Figure 4.*1(a), The HTFET with an InP drain (as mentioned in chapter three Figure *3.5*) achieves a higher ON-current primarily due to the high electron mobility and elevated electron concentration provided by the InP material. These properties enhance carrier transport by enabling efficient transfer of charge carriers from the valence band of the source to the conduction band of the channel, thereby improving band-to-band tunneling efficiency. Additionally, the optimal band alignment between InP and the channel material reduces the tunneling barrier, contributing to increased drive current.

The InP_Drain_HTFET also exhibits a stronger peak electric field as shown in figure 4.1(b) at the tunneling junction, which further reduces the tunneling barrier width and enables a greater number of electrons to tunnel from the source to the drain. This results in a significantly higher ON-current and improved conduction when the device is in the ON-state, highlighting its potential for superior performance in low-power, high-sensitivity applications.

Moreover, as depicted from the figure 4.1(c), InP_Drain_HTFET demonstrates superior carrier generation capability compared to conventional Si-based TFETs, as evidenced by a notable negative recombination rate observed in specific regions of the device. This is attributed to the direct band gap nature of InP, which facilitates radiative recombination, a process where electrons and holes recombine and emit photons. In contrast, the Conventional_TFET based on silicon (mentioned in *figure 3.4)*, an indirect band gap material, exhibits minimal and more stable recombination activity. While this may result in lower carrier generation efficiency, it could offer advantages in terms of device stability and reduced noise.

.

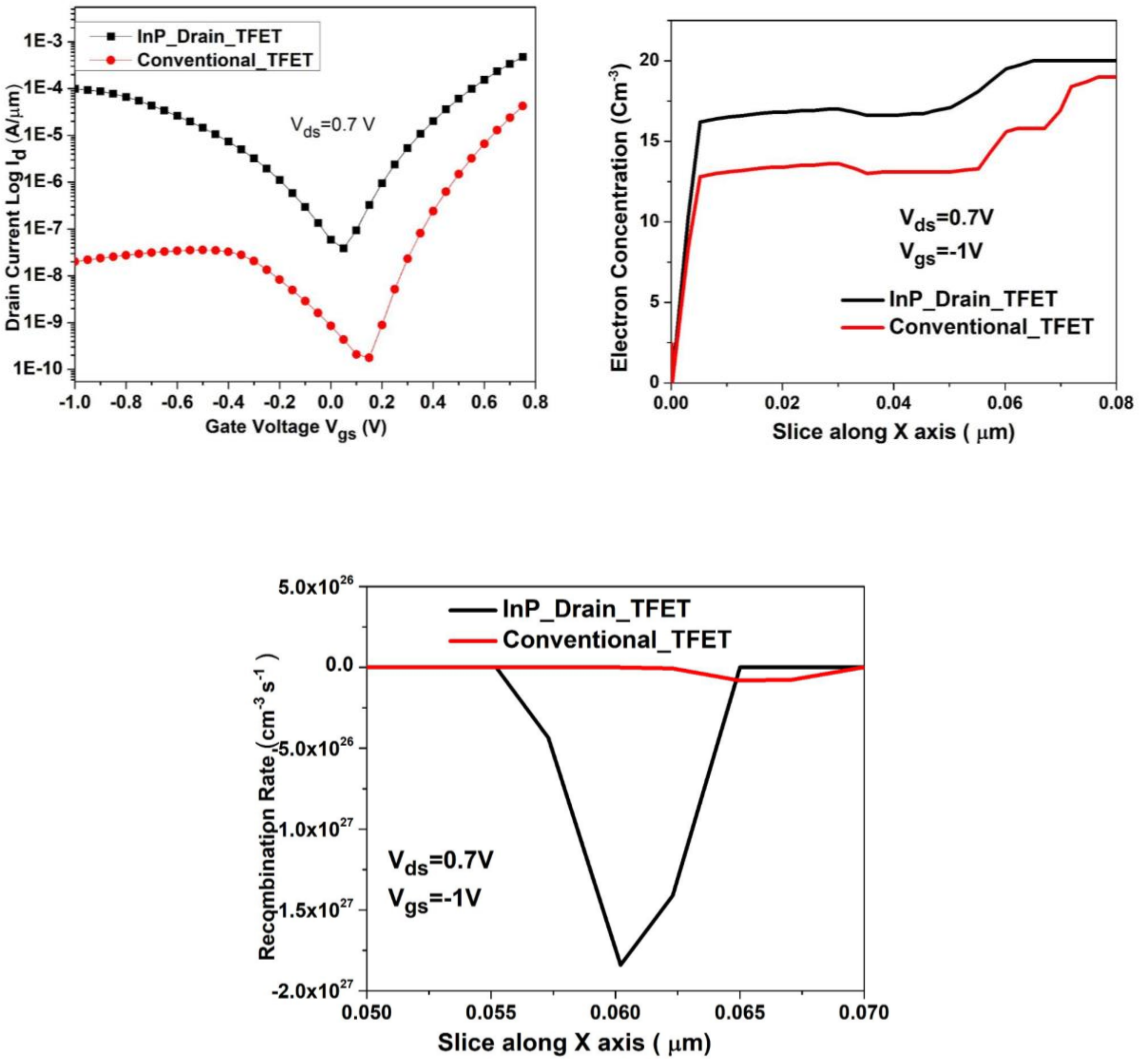


*Figure 4.1 Impact of InP-Drain on Source-Extended Heterostructure TFET a) Transfer characteristics (b)Electron Concentration (c) Recombination Rate*

## 4.2 Impact of Ge and InSb source on Source Extended HTFET

### 4.2.1 Indium Phosphide (InP) drain on Ge and InSb Source materials

The Ge source with InP drain-based HTFET (mentioned in *Figure 3.9* in chapter three) demonstrates lower leakage current and a more uniform and comparable electron concentration beyond the 0.04 µm slice, indicating better leakage control and carrier stability across the channel as shown in *Figure 4.2(a)*. When the Ge Source compared with InSb source with InP drain HTFET. It is observed that Ge offers better control over ambipolar conduction although InSb achieves a comparable ON-current. This performance is because of InSb narrower bandgap, lower effective mass, and higher intrinsic electron concentration compared to Ge as observed in figure 4.2(b). Furthermore, InSb direct bandgap enables efficient carrier injection even at low gate voltages, making it particularly suitable for ultra-low-power applications despite its higher leakage characteristics.

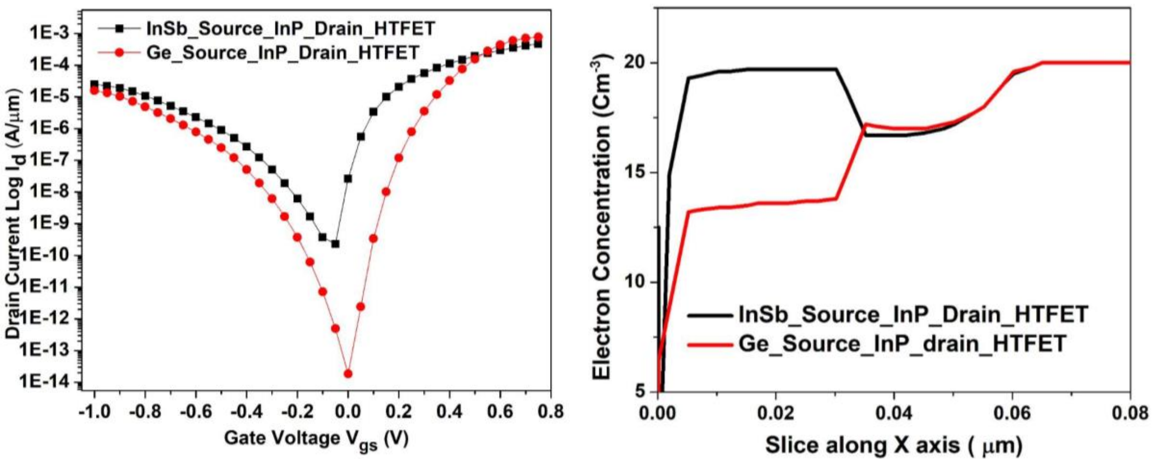


*Figure 4.2 Impact of InP-Drain on Ge and InSb Source a) Transfer characteristics (b)Electron Concentration*

As depicted in *Figure 4.3(a),* a comparative analysis between HTFETs using an InSb source/Ge Source (mentioned in *Figure 3.8* in the previous chapter) with an InP drain reveals significant differences in electrostatic behavior and overall device performance. The superior electronic properties of InSb specifically, its higher electron mobility, lower effective mass, and direct bandgap are not only responsible for achieving higher ON-current and increased electron concentration, but also contribute to a higher overall potential near the source-channel junction compared to the Ge-based device.

The sharper potential drop in the InSb-based HTFET indicates a stronger electric field at the tunneling junction, which greatly enhances band-to-band tunneling (BTBT) mechanism. Furthermore, the impact of Ge source and InSb source on total current density is shown in figure 4.3(b). Due to the lower band gap of InSb, the current density seems more but there is no significant increment due to material specific transport limitations. Due to this much advantages of InSb material over others, it supports efficient tunneling and make InSb highly suitable for high-speed, low-power applications, as well as infrared detection technologies.

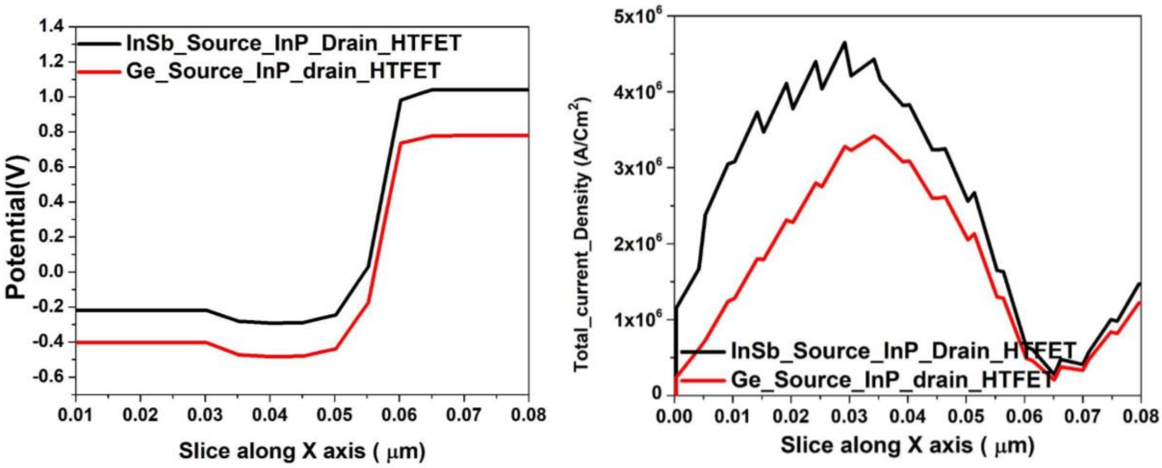


*Figure 4.3 Impact of InP-Drain on Ge and InSb Source c) Potential Comparison (d)Total Current Density*

### 4.2.2 Silicon (Si) drain on Ge and InSb Source materials

*Figure 4.4* illustrates the comparison of the ON-current in transfer characteristics (fig a), potential distribution (fig b), and total current density (fig c) between HTFETs with Ge and InSb sources paired with a Si drain (discussed at *Figure 3.7*), the Ge-source device demonstrates superior performance. This can be attributed to several critical factors. Firstly, band alignment between Ge and Si offers a more favorable tunneling junction due to a relatively smaller conduction band offset, which facilitates smoother carrier injection across the source-channel interface. Although InSb has a narrower bandgap and higher electron mobility, its band alignment with Si is less optimal, leading to reduced tunneling probability.

Additionally, tunneling probability in the Ge/Si configuration (mentioned at *Figure 3.7*) is enhanced by the better band overlap and a more controlled electric field profile, which increases the effective tunneling window. Carrier mobility, though higher in InSb, is less influential in this scenario due to the dominant role of tunneling mechanisms in the ON-state current.

Moreover, it has better lattice compatibility with Si, reducing defect density and improving interface quality, which is critical for maintaining device reliability and minimizing leakage. In contrast, the significant lattice mismatch between InSb and Si can introduce interface states and dislocations, adversely affect carrier transport and tunnel efficiency.

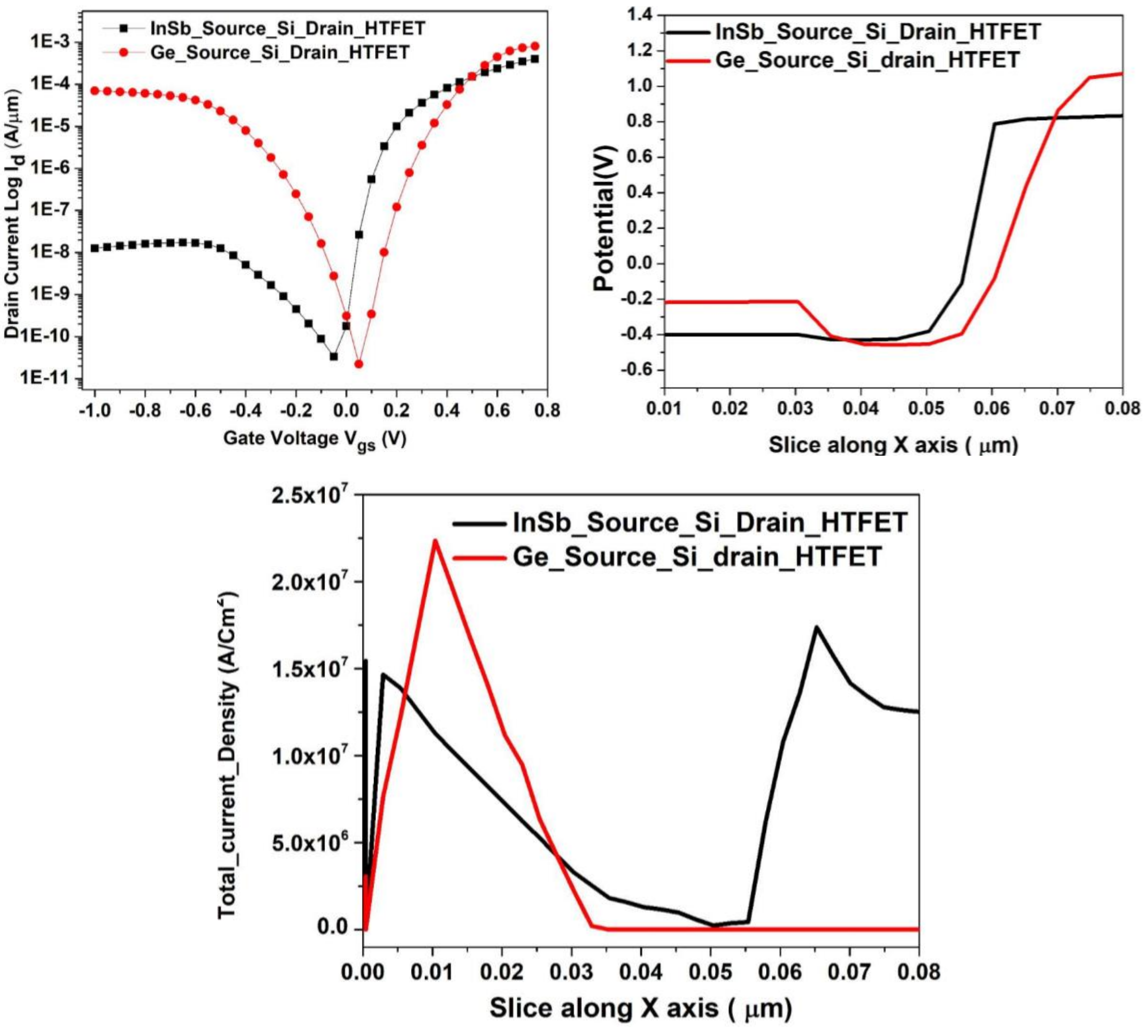


*Figure 4.4 Impact of Si -Drain on Ge and InSb Source a) Transfer characteristics (b)Potential (c)Total Current Density*

### 4.2.3 Germanium Split Source on source Extended Heterostructure TFET

As shown in *Figure 4.5*, a comparison between HTFETs utilizing a Ge split (or finger) source (shown at *Figure 3.10* (and a full Ge source with an InP drain (shown at *Figure 3.9*) reveals that the split source configuration delivers superior performance. Although both devices employ InP as the drain material, the split Ge source exhibits enhanced ON-state current as shown in fig 4.5 (a), electric field intensity (fig 4.5 (b), potential distribution (fig 4.5 c), and total current density fig 4.5(d).

This improvement is primarily attributed to the split source design, which facilitates a combination of point, line, and diagonal tunneling mechanisms. These multiple tunneling paths enhance the tunneling probability across the source-channel junction, resulting in a stronger electric field and more efficient carrier injection. As a result, the split Ge source significantly boosts the overall current conduction and device performance compared to the conventional full Ge source configuration.

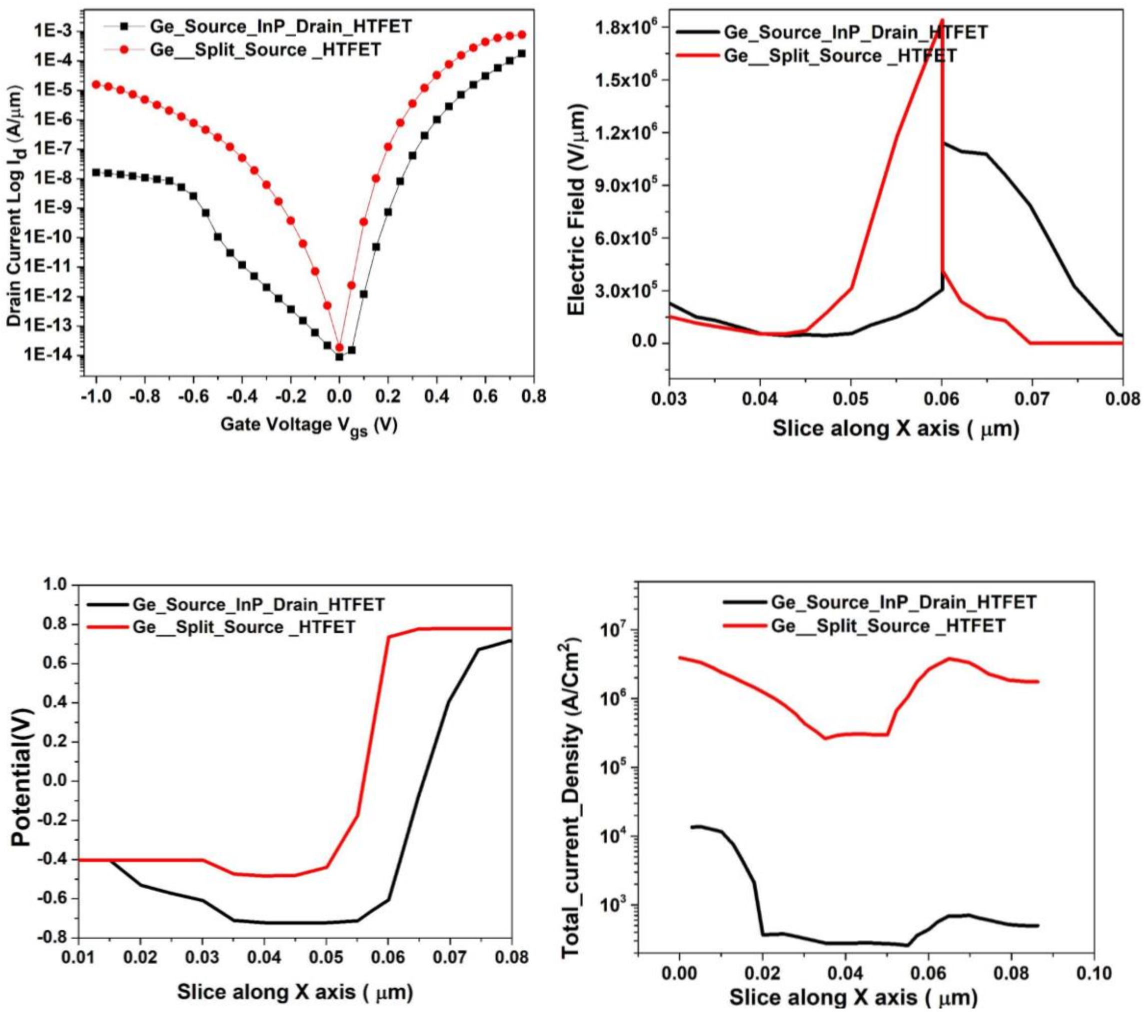


*Figure 4.5 Impact of Ge Split -Source on InP Drain a) Transfer characteristics (b)Electric Field (c)Potential (d)Total Current Density*

## 4.3 Analysis of Modified Conventional Heterostructure TFET

### 4.3.1 Transfer Characteristics of the Modified Conventional TFET with Dielectric Pocket

As illustrated in the *Figure 4.6,* when we are utilizing the $HfO_2$ as the dielectric pocket on the drain side in the conventional TFET it demonstrates superior performance in terms of leakage current suppression and ambipolar behavior control. Under OFF-state conditions (zero gate voltage and positive drain voltage), $HfO_2$ shows the lowest drain current as compared to $SiO_2$ and $Si_3N_4$. Additionally, under negative gate bias where ambipolar conduction is prominent

$HfO_2$ exhibits the lowest ambipolar current, effectively minimizing reverse leakage. While all three dielectrics show comparable ON-state currents at high gate voltages, these results suggest that $HfO_2$ offers a distinct advantage in reducing unwanted leakage and ambipolar effects, which are critical for energy-efficient TFET operation.

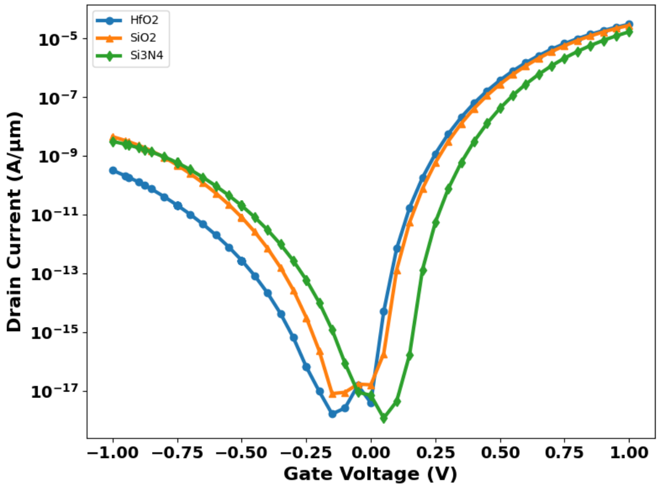


*Figure 4.6 Variation of transfer characteristics Comparison of Different Dielectric pockets (DP) on TFET*

*Figure 4.7* presents a comparative analysis of three horizontally structured HTFET devices utilizing InAs as the source and InP as the channel and drain (mentioned at *Figure 3.12*). The first structure incorporates a dielectric pocket (DP) (discussed at *Figure 3.13*) near the drain region using a different k material, which helps in reducing the ambipolar current while the second integrates an InSb source pocket (SP) between the source and channel (shown at *Figure 3.14*). The source pocket generally we are utilized to enhance the drive capability of the device. And the third figure in which we combine both pockets (at drain side and at source side) for optimized performance (described a *Figure 3.15*).

In the dielectric pocket HTFET, the primary goal is to suppress ambipolar conduction and reduce leakage current under negative gate bias. The high-k dielectric reshapes the electric field near the drain, forming an effective tunneling barrier that impedes reverse carrier injection. Although this structure improves OFF-state control and reduces leakage, it maintains a similar ON-current to the conventional design, indicating that source-side tunneling remains unaffected by the drain-side modification. In contrast, the source-pocketed HTFET with an InSb region significantly improves ON-state current due to enhanced band-to-band tunneling

(BTBT) at the source-channel interface. The narrower bandgap of InSb increases tunneling probability, leading to higher drive current. Additionally, it exhibits sharper subthreshold swing and partial suppression of ambipolar conduction, offering better gate control compared to the baseline device. However, it still experiences some OFF-state leakage, as it lacks any drain-side tunneling barrier.

.

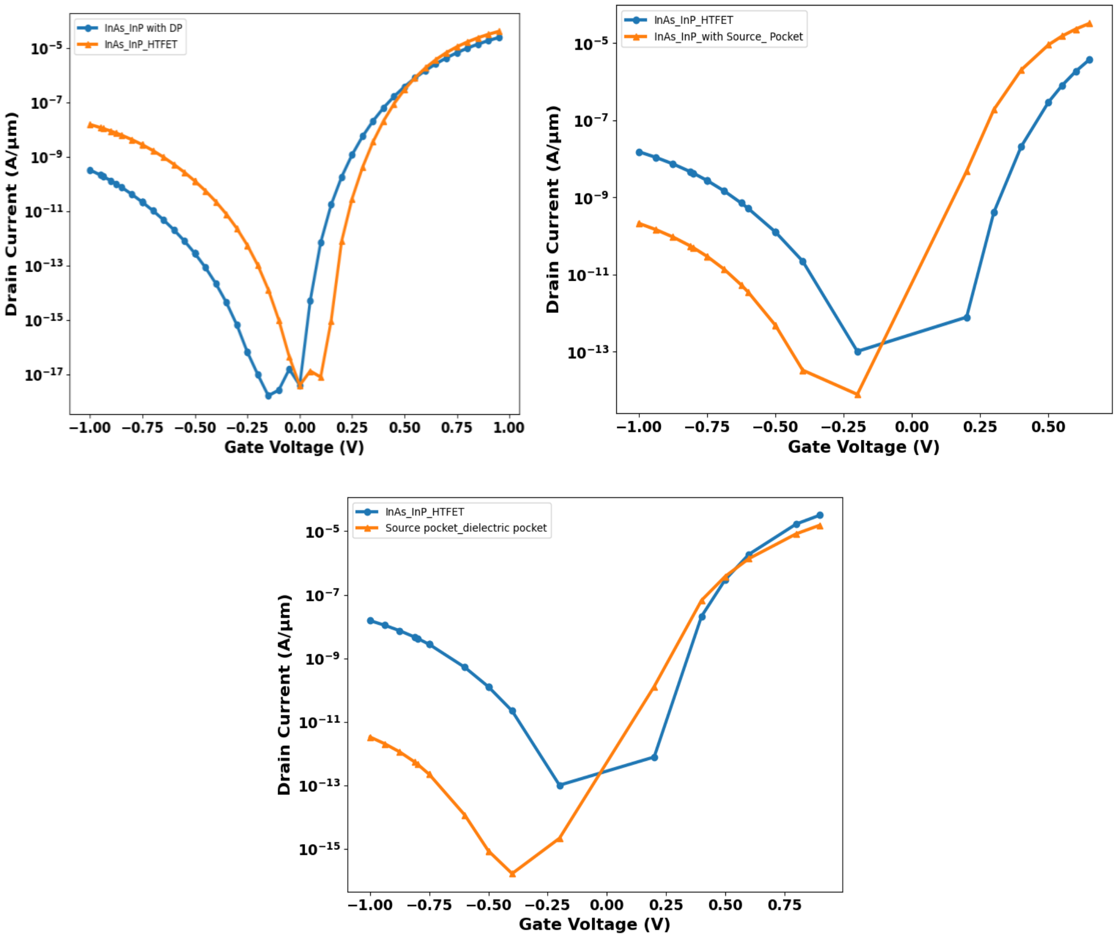


*Figure 4.7 Transfer characteristics (a)HTFET with DP (b) HTFET with SP (c) HTFET with both DP and Source Pocket (SP)*

The combined pocket HTFET, integrating both the InSb source pocket and the dielectric drain pocket, theoretically offers the most balanced and optimized performance. This design enhances ON-current via efficient source-side tunneling while effectively reducing leakage and ambipolar current through drain-side suppression. It also achieves the steepest subthreshold swing, making it highly suitable for low-power, high-performance applications. These modifications are not only intended to overcome the intrinsic shortcomings of conventional TFETs but also to optimize the trade-offs among key performance metrics such as ON-current (ION), OFF-current (IOFF), and subthreshold swing (SS). Through systematic device simulation and analysis, the effects of each individual modification and combinations thereof are carefully evaluated. The transfer characteristics, including I–V curves, SS values, and leakage behavior, are compared across different device configurations. Table 4.1 shows the comparison between the simulated proposed structures and the already published data by the

*Table 4.1 Comparison of proposed Device structure with already published results*

| Parameter | InP AND GaAs DOUBLE GATE MOSFET (Geege, A. S., et al. 2020) | Cylindrical Channel Gate All Around InGaAs/InP Heterojunction TFET ((Vimala et al., 2021). | Proposed Ge-Split-Source HTFET | Proposed InAs with InGaAs source pocket HTFET |
|---|---|---|---|---|
| On-state current(A/µm) | $10^{-3}$ A/µm | $10^{-5}$ A/µm | $1.768\text{x}10^{-4}$ | $4.227\text{x}10^{-4}$ |
| Off-state current(A/µm) | $10^{-11}$ A/µm | $10^{-12}$ A/µm | $8.974\text{x}10^{-15}$ | $5.035\text{x}10^{-14}$ |
| On -state/Off-state current ratio | $10^{8}$ | $10^{7}$ | $1.97\text{x}10^{10}$ | $8.395\text{x}10^{9}$ |

## 4.4 Proposed Heterojunction TFET structures as a Biosensors

This section explores the biosensor application of the proposed Ge-Split-Source HTFET using a dielectric-modulated sensing approach. The figure of the biosensor is shown in figure 3.1. A cavity is introduced in the gate region to host biomolecules, enabling label-free detection based on changes in dielectric properties. The biomolecules considered in this study are neutral, meaning they do not carry any charge and influence the device behavior solely through their permittivity. Further the vertical Heterostructure TFET structure which is discussed in figure 3.16 is utilized to realize the biosensor shown in figure 3.17. In this work, we used a $p^+$-InAs source and an InGaAs pocket at the source–channel interface of a vertical heterojunction TFET (HTFET). InAs was chosen primarily for its narrow bandgap and high electron mobility, which were crucial for enhancing device performance in low-power applications such as biosensing. The narrow bandgap of InAs reduced the tunneling barrier at the source–channel junction, enabling efficient band-to-band tunneling (BTBT) and resulting in a higher ON-current. Additionally, the high electron mobility improved post-tunneling carrier transport, contributing to faster switching and a steeper subthreshold swing, both of which were essential for low-power operation.

The biosensor utilized dielectric modulation, where the permittivity (k-value) of the material in the cavity region was varied to influence sensitivity. An increase in permittivity concentrated the electric field within the cavity, thereby enhancing the electrostatic coupling between the gate and channel. This stronger field further promoted BTBT in the HTFET structure, leading to an increase in drain current. While the use of InAs significantly improved both the ON-current and subthreshold swing, it was also observed that the ambipolar current decreased progressively with increasing dielectric permittivity. Among the performance metrics, the ON-current variation with different dielectric constants was found to be the most effective indicator of sensitivity and was therefore used as the key sensing parameter in our biosensor.

Furthermore, the high surface-to-volume ratio of the nanostructured device architecture provides additional active binding sites for biomolecules, further boosting the current response. As a result, variations in biomolecule presence are directly reflected in the device's transfer characteristics, establishing a clear link between drain current behavior and biosensing performance.

The sensitivity $S_I$ of the biosensor is calculated using the following expression:

$$SI = \frac{I_D(\text{bio}) - I_D(\text{air})}{I_D(\text{air})} \ldots\ldots\ldots\ldots\ldots.. \quad \text{Equation 4.1}$$

Here, $I_D$ (bio) is the drain current when biomolecules are present, and $I_D$ (air) is the drain current when the cavity is filled with air. This method aligns with the widely used dielectric modulation technique, one of the two common approaches in biosensing, alongside the gating technique. By focusing on dielectric property variations, the proposed HTFET-based biosensors offer a sensitive and low-power platform for real-time biomolecule detection.

**Variation of Transfer Characteristics ($I_D$–$V_{GS}$) for different k values**

In this work we have chosen four biomolecules i.e., streptavidin (k=2.1) Feroocytochrom (k=5.1), keratin (k=8) and gelatin (k=12). Figure 4.8 (a) demonstrates the change in drain current when the permittivity of various biomolecule is modulating in vertical HTFET with InAs Source and InGaAs pocket. Figure 4.8 (b) depicts the impact of immobilization of different biomolecule on the transfer characteristics for Ge-Split-Source HTFET Biosensor. As it is observed that the device's drain current increases as the cavity's permittivity rises. The permittivity of the cavity, sensing region, or active region in a biosensor influences the device's sensitivity since it dictates how the capacitance structure is sensed, which is usually impacted by biomolecules presence.

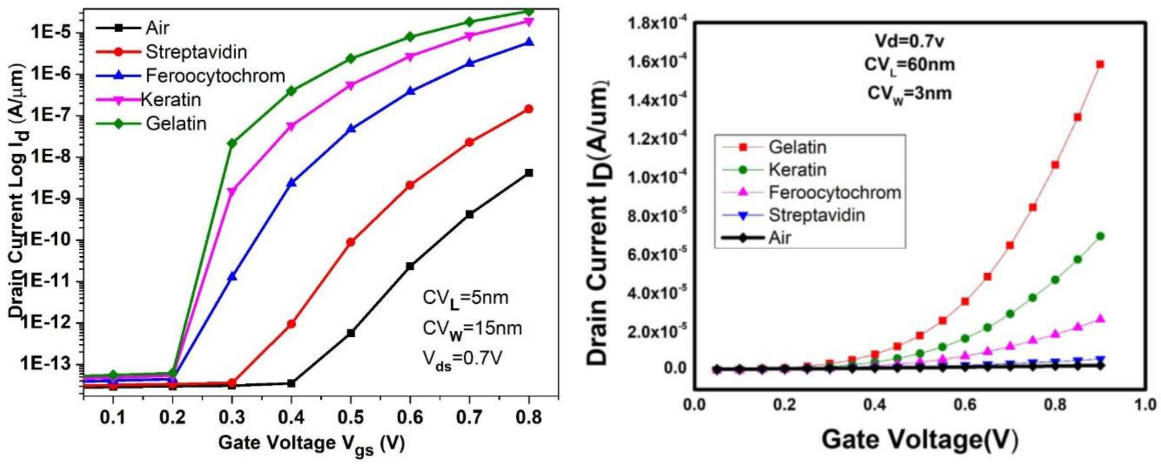


*Figure 4.8 Transfer characteristics (a)Proposed InAs with InGaAs pocket Biosensor (b) Proposed Ge-Split-Source HTFET Biosensor*

Because of the interaction with the biomolecules, the capacitance changes as the cavity's permittivity rises. The change in drain current is a result of this capacitance variation. Figure 4.8 displays a high ON current at k=12. The cavity's permittivity and electric field have a direct proportional effect; as the permittivity rises, the electric field also rises as shown in figure 4.9. This relationship can be expressed as follows:

$$E \propto V/\,(\epsilon * d),$$

Where:

- E = Electric field intensity (V/m)
- V = Applied voltage or potential difference (V)
- ε = Dielectric constant (absolute permittivity) of the material (F/m)
- d = Distance or effective thickness of the dielectric region (m)

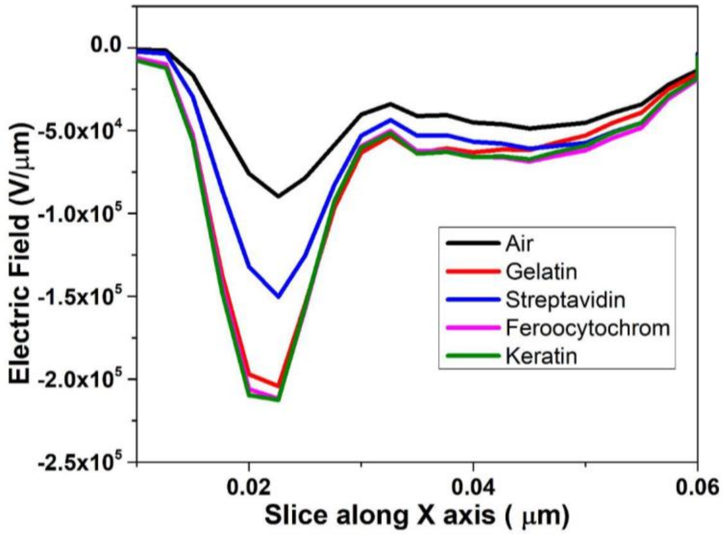


*Figure 4.9 Electric Field for Proposed Ge-Split-Source HTFET Biosensor*

Because of the difference in permittivity, the electric fields change even when the same voltage is applied. This relationship is beneficial because it raises capacitance; the stronger the field, the higher the capacitance in the tea cavity region, which affects the device's overall electrical performance and charge storage capacity. Figure 4.9 provides an illustration of those principles.

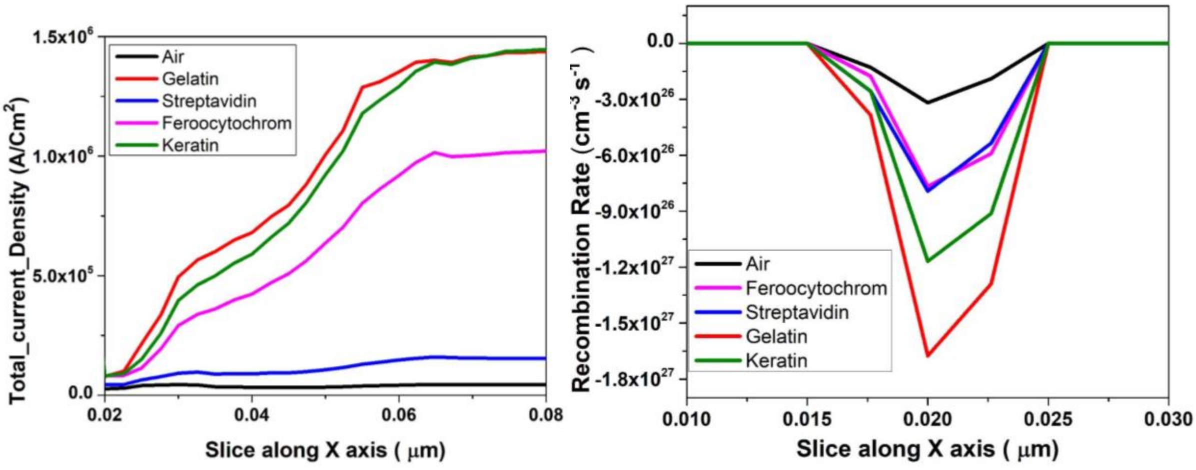


*Figure 4.10 Proposed Ge-Split-Source HTFET Biosensor (a)Total Current Density(b)Recombination Rate*

In the above *Figure 4.10* illustrates how carrier injection, electric field strength, and material characteristics affect the total current density, the total current density in a biosensor relies on the movement of charge carriers, such as electron, in the sensing region or cavity. An increase in gate capacitance due to a larger dielectric constant intensifies the electric field at the tunneling junction, improving band-to-band tunneling (BTBT) and raising the ON-current.

Furthermore, an optimal doping concentration lowers the energy barrier, which encourages carrier injection and raises the current density even more. The dielectric environment also affects the recombination rate; a greater dielectric constant can increase carrier lifetime and tunneling efficiency by reducing undesired recombination and improving electrostatic control which is shown in figure 4.11(b). The major figure of merit for any biosensor is the sensitivity. In both the proposed device biosensor we are utilizing the $I_{on}$ current as the sensitivity parameter. To avoid the more signal to noise ratio in the FET based biosensor generally we operate the biosensor at the lower drain voltage.

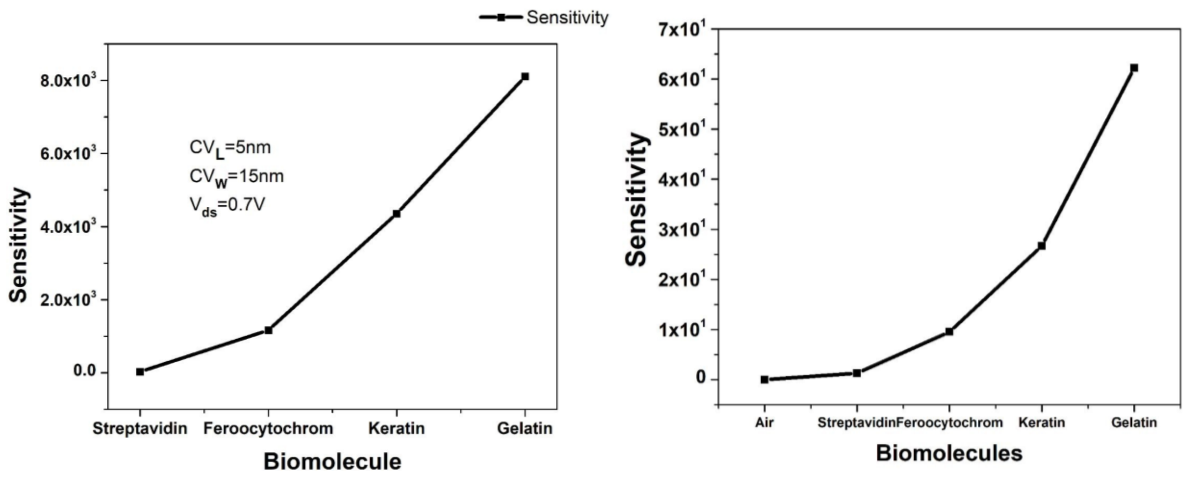


*Figure 4.11 Sensitivity of (a) Proposed InAs with InGaAs pocket Biosensor (b) Proposed Ge-Split-Source HTFET Biosensor*

Figure 4.11 (a) shows the sensitivity for the particular biomolecules when it immobilizes inside the cavity region in InAs with InGaAs pocket biosensor. Similarly in figure 4.11 (b) it depicts for the Ge-Split Source HTFET biosensor. The figure shows that the proposed InAs device with an InGaAs pocket source exhibits higher sensitivity compared to the proposed Ge-Split Source HTFET biosensor. This is due to the fact that in that case the surface to volume ratio is more and the value of Ion is comparatively less than the other case. *Figure 4.12* the comparison between the two proposed structures is given in the form of bar diagram. Out of them two structures the sensitivity of Proposed InAs with InGaAs pocket Biosensor is best for all the neutral biomolecules. This is due to key variations in material characteristics, cavity design, doping profiles, and field modulation are responsible for the InAs with InGaAs Pocket biosensor's higher sensitivity compared to the Ge Split-Source HTFET biosensor. A greater interaction volume for biomolecules is provided by the structurally longer cavity length (15 nm) of the InAs-based biosensor as opposed to the Ge-based device's 3 nm. Furthermore, the InAs device's smaller cavity width (5 nm) results in a higher electric field concentration, which intensifies the dielectric influence of biomolecules on the tunneling barrier. Wider cavities can increase sensitivity, but they can also increase steric hindrance, which makes it harder for biomolecules to get to the sensing area.

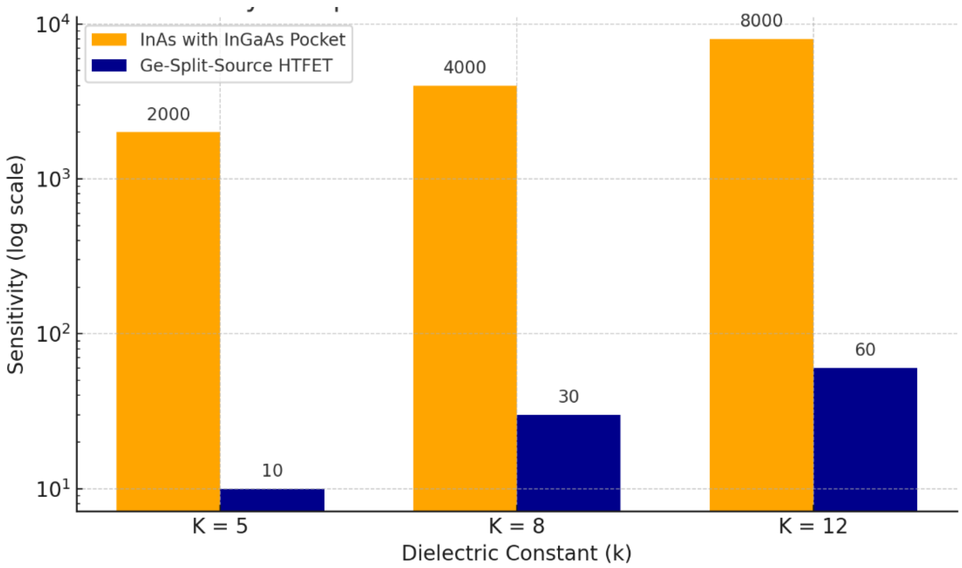


*Figure 4.12 Sensitivity Comparison between the two proposed structures i.e., Proposed InAs with InGaAs pocket Biosensor and Proposed Ge-Split-Source HTFET Biosensor*

The InAs/InGaAs biosensor's ultra-lightly doped channel ($1 \times 10^{12}$ $cm^{-3}$) increases sensitivity to dielectric manipulation and enhances gate electrostatic control. Effective carrier transport is facilitated by its low effective mass, strong electron mobility, and reduced bandgap. Furthermore, although heterojunctions are used in both devices, the InAs/InGaAs heterojunction, which is located at the source channel interface, is essential for improving band-to-band tunneling (BTBT) efficiency.

By leveraging the benefits of heterojunction engineering and vertical current transport, HTFETs present a promising solution for energy-efficient, high-performance applications particularly in the fields of biosensing. This section lays the groundwork for understanding their structural strengths, operating mechanisms, and material selection strategies relevant to biosensor optimization.

# CHAPTER 5 CONCLUSION AND RECOMMENDATIONS

## 5.1 Conclusion

This study explored two major heterojunction TFET architectures optimized for low-power applications. The Ge Split-Source HTFET architecture leverages a combination of point, line, and diagonal tunneling mechanisms. This results in a significantly improved ON-state current of $1.758\times10^{-4}$ A/µm, a high Ion/Ioff ratio of $1.974\times10^{10}$, and a sharp subthreshold swing (SS) of 18.7 mV/dec. In contrast, the Vertical Heterojunction TFET (V-HTFET) structure featuring an InAs source and InGaAs pocket exploits the low bandgap and effective mass of InAs to boost tunneling probability. The moderate bandgap and favorable band alignment of InGaAs further enhance device performance, achieving an ON-current of $4.201\times10^{-4}$ A/µm and an Ion/Ioff ratio of $8.385\times10^{9}$.

Two biosensor architectures Ge Split-Source HTFET Biosensor and InAs/InGaAs Pocket HTFET Biosensor were evaluated for their potential in biosensing applications. Both designs were optimized for enhanced tunneling efficiency and sensitivity. A variety of biomolecules, including streptavidin, ferricytochrome, keratin, and gelatin, were introduced into the sensing chamber to assess biosensing performance. Measurements were conducted at a drain-source voltage (VDS) of 0.7 V under controlled conditions. Critical structural parameters such as sensing cavity position, dimensions, and biomolecule placement were analyzed. It was observed that biomolecules placed closer to the tunneling junction led to higher sensitivity, due to stronger modulation of the local electric field. When comparing both designs, the InAs/InGaAs HTFET biosensor demonstrated superior performance in terms of drain current sensitivity and ON-state current, aligning well with trends observed in recent literature.

The study demonstrates that heterojunction TFETs, particularly those utilizing InAs/InGaAs material systems, hold strong potential for low-power, high-sensitivity biosensing applications. The combination of optimized tunneling junctions, careful material selection, band alignment engineering, and precise sensing cavity design enables the realization of next-generation TFET-based biosensors. These findings contribute to the growing body of research aimed at developing energy-efficient, high-performance, and scalable biosensing platforms for applications in healthcare, environmental monitoring, and point-of-care diagnostics.

## 5.2 Recommendations

Building on the outcomes of this study, future research can explore several directions to further enhance the performance and practical implementation of TFET-based biosensors:

1. **Charge-Based Biomolecule Detection:** While neutral biomolecules were the focus of this work, next research might examine the effects of charged biomolecules, allowing detection based on both electrostatic contact and dielectric modification, which could increase sensitivity and selectivity
2. **Noise and Reliability Analysis:** Incorporating noise analysis, process variation, and long-term reliability studies would provide deeper insights into the sensor's behavior in real operating environments
3. **Experimental Validation**: Although simulation findings from the suggested designs have been encouraging, experimental fabrication and testing are necessary to confirm the InAs/InGaAs biosensor's viability, repeatability, and resilience in the real world.
4. **Integration with CMOS Technology:** For scalable and economical deployment in portable diagnostic systems, it would be essential to look at the co-integration and compatibility of the suggested TFET biosensors with current CMOS platforms.

## REFERENCES

Ahish, S., Sharma, D., Vasantha, M. H., & Kumar, Y. B. N. (2016). Design and analysis of novel InSb/Si heterojunction double gate tunnel field effect transistor. *2016 IEEE Computer Society Annual Symposium on VLSI (ISVLSI)*, 105–109. https://doi.org/10.1109/ISVLSI.2016.52

Ahish, S., Sharma, D., Vasantha, M. H., & Kumar, Y. B. N. (2017). Performance analysis of InGaAs/GaAsP heterojunction double gate tunnel field effect transistor. *Superlattices and Microstructures*, *103*, 93–101. https://doi.org/10.1016/j.spmi.2017.01.014

Bergveld, P., Hendrikse, J., & Olthuis, W. (1998). Theory and application of the material work function  for chemical sensors based on the field effect principle. *Measurement Science and Technology*, *9*(11), 1801. https://doi.org/10.1088/0957-0233/9/11/003

Bhattacharyya, A., Chanda, M., & De, D. (2019). Performance Assessment of New Dual-Pocket Vertical Heterostructure Tunnel FET-Based Biosensor Considering Steric Hindrance Issue. *IEEE Transactions on Electron Devices*, *66*(9), 3988–3993. https://doi.org/10.1109/TED.2019.2928850

Datta, E., Chattopadhyay, A., Mallik, A., & Omura, Y. (2020). Temperature Dependence of Analog Performance, Linearity, and Harmonic Distortion for a Ge-Source Tunnel FET. *IEEE Transactions on Electron Devices*, *PP*, 1–6. https://doi.org/10.1109/TED.2020.2968633

Dewan, B., Chaudhary, S., Singh, D., & Yadav, M. (2024). Label-free detection of breast cancer cell lines using dopingless heterojunction TFET considering non-ideal hybridization issue. *Materials Science and Engineering: B*, *302*, 117192. https://doi.org/10.1016/j.mseb.2024.117192

Farkoush, B. A., & Dideban, D. (2020). Investigating the Source Stack Engineering Effect on the Drive Current of a Tunneling Field Effect Transistor. *Silicon*, *12*(11), 2733–2740. https://doi.org/10.1007/s12633-019-00371-7

Ghadimi Avval, A., Larique, E., & El-Ghazaly, S. M. (2018). Heterojunction Field-Effect Transistors. In *Reference Module in Materials Science and Materials Engineering*. Elsevier. https://doi.org/10.1016/B978-0-12-803581-8.11349-9

Hamza, M., Goel, R., Verma, M., & Agrawal, S. (2112). *Comparative Analysis of Dual Metal Gate-Split Source and Single Source Bilateral Tunnel Field Effect Transistor*.

Hong, S., Lee, J., Kim, D., & Park, S. (2021). FET-based gas sensors: Challenges and opportunities. *Journal of Materials Chemistry C*, *9*(5), 1532–1548.

https://doi.org/10.1039/D0TC04459G

Hossain, N., Rimon, M. I. H., Mimona, M. A., Mobarak, M. H., Ghosh, J., Islam, Md. A., & Al Mahmud, Md. Z. (2024). Prospects and challenges of sensor materials: A comprehensive review. *E-Prime – Advances in Electrical Engineering, Electronics and Energy*, 100496. https://doi.org/10.1016/j.prime.2024.100496

Karthik, K. R. N., & Pandey, C. K. (2023). A Review of Tunnel Field-Effect Transistors for Improved ON-State Behaviour. *Silicon*, *15*(1), 1–23. https://doi.org/10.1007/s12633-022-02028-4

Kumar, Ch. P., & Sivani, K. (2016). A tunnel field effect transistor is a substitute for ultra-low power applications. *2016 International Conference on Advances in Human Machine Interaction (HMI)*, 1–4. https://doi.org/10.1109/HMI.2016.7449164

Liu, Y., Xiao, S., & Du, K. (2021). Chemiresistive Gas Sensors Based on Hollow Heterojunction: A Review. In *Advanced Materials Interfaces* (Vol. 8, Issue 12). John Wiley and Sons Inc. https://doi.org/10.1002/admi.202002122

Poorna Sundari, M., & Lakshmi Priya, G. (2024). Nano-biosensors with subthreshold swing tunnel field effect transistor: A cutting-edge review. *Sensing and Bio-Sensing Research*, *44*, 100665. https://doi.org/10.1016/j.sbsr.2024.100665

Reddy, N. N., & Panda, D. K. (2020). Tunnel field-effect transistor-based biosensors: A review. *Silicon*, *12*(7), 1545–1558. https://doi.org/10.1007/s12633-020-00657-1

Santa Clara, C. (2004). *ATLAS User's Manual DEVICE SIMULATION SOFTWARE*. www.silvaco.com

Saravanan, M., Parthasarathy, E., & Ramkumar, K. (2022). Performance analysis of InAs-GaAs gate-all-around tunnel field effect transistors (GAA-TFET) for analog/RF applications. *Journal of Physics: Conference Series*, *2335*(1), 12043. https://doi.org/10.1088/1742-6596/2335/1/012043

Swain, S. K., Malviya, N., Singh, S., & Sharma, S. K. (2021). InSb/Si heterojunction-based tunnelling field-effect transistor with enhanced drive current and steep switching. *Journal of Electronic Materials*, *50*(12), 6765–6774. https://doi.org/10.1007/s11664-021-09325-5

Swati, Kaur, J., & Singh, A. K. (2023). Performance investigation of an InAs-based dielectric-modulated heterojunction TFET as a label-free biosensor. *Applied Physics A: Materials Science and Processing*, *129*, 365. https://doi.org/10.1007/s00339-023-06643-9

Theja, A., & Panchore, M. (2023). Vertically developed double gate GaSb/Si based tunnel field effect transistor as a label-free biosensor: A simulation study. *IEEE Transactions on Nanobioscience*, *22*(2), 284–291. https://doi.org/10.1109/TNB.2022.3196687

Tiwari, S., & Saha, R. (2022). Methods to Reduce Ambipolar Current of Various TFET Structures: a Review. *Silicon*, *14*(12), 6507–6515. https://doi.org/10.1007/s12633-021-01458-w

Verreck, D., Groeseneken, G., & Verhulst, A. (2016). The Tunnel Field-Effect Transistor. In *Wiley Encyclopedia of Electrical and Electronics Engineering* (pp. 1–24). Wiley. https://doi.org/10.1002/047134608x.w8333

Vimala, P., Sampath, N. G. H., & Priyadarshini, N. D. (2021). Boosting on current using various source material for dual gate tunnel field effect transistor. *Journal of Nanotechnology and Nano-Engineering*, *7*(1–2), 1–6. https://doi.org/10.46610/JONNE.2021.v07i01.001

## Research Fund Acknowledgement

This research is funded by Adama Science and Technology University under the grant number ASTU/SM-R/1127/25, Adama, Ethiopia.